MPI Informatics Building Model as Data for Your Research

Vlastimil Havran, Jozef Zajac,
Jiří Drahokoupil, Hans-Peter Seidel

MPI–I–2009–4–004 December 2009

Authors' Addresses

Vlastimil Havran
Department of Computer Graphics and Interaction
Czech Technical University in Prague
Czech Republic

Jozef Zajac
Slovakia

Jiří Drahokoupil
Department of Computer Graphics and Interaction
Czech Technical University in Prague
Czech Republic

Hans-Peter Seidel
Max-Planck-Institut für Informatik
Saarbrücken, Germany

Abstract

In this report we describe the MPI Informatics building model that provides the data of the Max-Planck-Institut für Informatik (MPII) building. We present our motivation for this work and its relationship to reproducibility of a scientific research. We describe the dataset acquisition and creation including geometry, luminaires, surface reflectances, reference photographs etc. needed to use this model in testing of algorithms. The created dataset can be used in computer graphics and beyond, in particular in global illumination algorithms with focus on realistic and predictive image synthesis. Outside of computer graphics, it can be used as general source of real world geometry with an existing counterpart and hence also suitable for computer vision.

Keywords

reference dataset, building model, geometric data, research reproducibility, predictive image synthesis, global illumination, validation.

Contents

1 Introduction

Geometric and non-trivial datasets are needed not only in computer graphics research. However, particularly in computer graphics, in the field of global illumination algorithms, there is a rising demand for scenes with visual complexity approaching the real world. As an example the predictive image synthesis [12] aims for algorithms, where the resulting image/video is hardly distinguishable from the reality. There are only a few datasets created according to the real world scenes that allow us to validate the capability of lighting simulation programs. Many other created datasets do not resemble the real world environment and/or their complexity is insufficient, and/or they miss the real world counterpart. The need for more complex datasets resembling reality for testing algorithms is evident in the field of geometric algorithms and computer graphics, which includes range searching, spatial data structures, and various simulation based on these problems such as light, sound, and radio signals propagation. If the dataset is sufficiently close to the real world, it allows us to experimentally validate the computed results against the data measured in the real world environment. Conversely, computer vision aims to reconstruct 3D models from captured or computed images/videos that should be compared against the reference data. These validations are rarely carried out because of the lack and accessibility of suitable reference datasets.

In this report we describe our effort to create a dataset corresponding to medium to large scale building of Max-Planck-Institut für Informatik in Saarbrücken, with seven floors, hundreds of offices and luminaires, and an interior atrium (see Figure 1.1) that forms highly complex visual effects. As the model was prepared with high level of detail and accuracy, we believe it can be used for a period of time as de facto standard case for experimental testing and validation of algorithms in computer graphics, computer vision, and other classes of computational problems. The dataset is publicly available in text formats including the ISO Standard format (VRML 97 according to ISO/IEC 14772-1:1997) to allow for its easy use and conversion

Figure 1.1: The rendered image from the MPI Informatics building model, computed by ray tracing with PBRT software.

in the future.

This research report is accompanied by a website that contains the dataset in version 1.0 at the website with URL[1]:

http://www.mpi-inf.mpg.de/resources/mpimodel/v1.0/

The structure of the research report is as follows. In Chapter 2 we discuss the reproducibility of research work with experimental results with respect to the availability of datasets used. In Chapter 3 we show the previous work on predictive image synthesis and lighting research with respect to created datasets models and methodology. In Chapter 4 we recall available datasets used in computer graphics with focus on global illumination. In Chapter 5 we describe the dataset we created. In Chapter 6 we discuss the problems we met and the limitation of the created dataset. Chapter 7 concludes the report with the prospects for future work.

[1]The future versions of the model will be located similarly, with the main webpage pointed on the address http://www.mpi-inf.mpg.de/resources/mpimodel/.

2 Reproducibility of Research Work

In this chapter we describe the relationship between the reproducibility of a research work in the context of experimental algorithmic research, where the results are dependent on the datasets used to evaluate a newly presented method.

2.1 Reproducibility

Reproducibility is a key property of any scientific research. It is stated that a research work is conditioned so if its results can be reproduced by any followers independently. This claim deals with completeness of description of a newly presented method. Let us quote e.g. the Internet encyclopedia, Wikipedia [40]:

> Reproducibility is one of the main principles of the scientific method, and refers to the ability of a test or experiment to be accurately reproduced, or replicated, by someone else working independently.

Similarly, the reproducibility is naturally required as a part of the scientific practice at universities and research institutes. Below we quote the text from Max-Planck-Society research guidelines [23]:

> The primary test of a scientific result is its reproducibility. The more surprising, but also the more desirable a result is, the more important it is - as far as is possible with justifiable expense or effort - that the route to that result be independently repeated within the research group before the result are passed on to the outside.

Now let us relate reproducibility to the experimental algorithmic research, which is indisputably dependent on the dataset that is used in evaluation, testing, and validation. This includes much of the research in computer graphics and computer vision; there is a strong dependence of results on the datasets used. The datasets mostly used in computer simulation can be characterized by different means, describing some measure of difficulty working with the data, often referred to as a *complexity* and it can be one or more of the following properties:

- size as the number of items,
- data dimensionality,
- data accuracy, possibly limited precision,
- statistical characterization as means, variance, etc.,
- characterization of information content, entropy, compressibility etc.

The list above is not (and cannot be) complete. In computer science size as the count of objects/entities is often used as it expresses minimum storage, but in our opinion this measure of complexity is overused in many cases.

As a newly presented algorithm is evaluated for some datasets by computing the results, the reproducibility of a published paper with the results requires to have an access to these datasets or to have a possibility to reproduce the datasets. The ability to reproduce a dataset, which is often difficult (and laborious) as it depends on many factors or personal choices (such as 3D modeling), is rather small and in fact impossible in practice. As an example we can take the geometric dataset from a car company for a particular car model. There is neither theoretical nor practical exact reproducibility of the dataset, even having the car physically available allows at most for creation of similar dataset (irrespective the time needed for this task), but definitely not the same. One reason is that the reality can be approximated by infinitely many different models with different accuracy. Another interesting algorithmic problem (and solved only partially) arising from this observation is to define and efficiently compute the measure of similarity provided by the two datasets.

Therefore we claim that the *real reproducibility* of a research paper presenting some experimental results requires availability of the datasets used for the experiments. As the private valuable datasets, often prepared by commercial subjects, are hard to reproduce or are not reproducible in practice, their use should be minimized or avoided. There are also other reasons, why the proprietary datasets should not be used:

- the authorship of a particular research is often recognizable even for a double-blind review of a paper to be reviewed. As the number of researchers (thus reviewers) in some research communities is small, there are (often publicly) known connections of some researchers to companies. Another detectable link is possible based on a known location of a company/well known product. Then it is relatively easy to identify the authorship of a submitted anonymous paper with quite a high certainty.

- in many cases some results from using private datasets can be shown (such as images, videos, performance results), but the dataset cannot be passed on to an independent researcher, be it either a collaborating or competing one. Often the dataset cannot be used after a project done in collaboration with a company is over, so the results cannot be reproduced by the researcher himself/herself (at least, not legally).

- the unavailability of private datasets in public disallows not only reproducibility, but also it disables indirect comparison when developing another method for the same or similar problem by an independent researcher, as the unavailable dataset cannot be used to create the results that could allow such indirect comparison.

Further, let us discuss how the availability of a dataset contributes to the validation of the implementation of an algorithm. Surely, having finished the algorithm implementation, we typically run the algorithms on an input available dataset. We compute the results, often the quantitative ones. There is a weak dependence - we can merely assume the correctness of an implementation of an algorithm - if the results of a re-implemented algorithm are equal with those of formerly published algorithm for the same input dataset. The strong claim is only in the opposite direction - when the results are different, then our implementation is not the same as the one described in the paper. In other words, the correctness of (re-)implemented algorithm cannot be enforced by using the (same) dataset and getting the same results. However, it is really useful to have a reference dataset available for comparing our implementation with a previous work. Even if we do not have the algorithms original implementation, based on the equality of the results we can assume our implementation is at least similar in properties and behaviour. Different implementation bugs can often be revealed by studying and comparing results against known values when running the algorithm against the dataset used in the original paper.

The procedure as described above reflects the scientific practice in computer graphics as of year 2009. It is worth to notice that within the last

decade it became almost necessary to compare results of a newly presented algorithm with those of formerly published papers, even if the implementations of the algorithms in the published papers are usually not available for different reasons. In practice it requires much re-implementation work and hence the use of the same datasets for testing these re-implementations can save significant amount of time.

3 Related Work in Computer Graphics and Lighting Research and Technology

In this chapter we want to survey the most important work related to the validation of rendering algorithms and the experimental datasets. There are in fact two research communities working partly independently that deal with computation of images. The first community is computer graphics and the second one is lighting research and technology. There is a number of papers related to problems of the computations for light transport. We want to point to a few surveys and to recall the most important related papers. Let us mention the survey report by Carrol [2] that provides the state of the art in 1999. A nice small introduction to photometry also for lighting engineers was provided by Ashdown [1]. Ulbricht et al. [36] surveyed the problems and results for predictive rendering from the perspective of computer graphics.

Below we discuss the particular work on validation and datasets focused on computer graphics, in particular predictive image synthesis, and lighting in roughly chronological order.

3.1 Radiometric and Visual Comparisons

The necessity to validate the results of global illumination against the real world data was recognized by Cindy M. Goral et al. by designing, reconstructing, and photographing a real cube [11] already in 1984. This work was extended by Cohen and Greenberg by the well-known Cornell Box [5] including radiometric comparisons by Mayer et al. [24]. Takagai et al. [34] used a car model to validate the result of a rendering algorithm against a ground truth image. Karner and Prantl [16] created a model of a simple office scene and compared the results from two rendering algorithms against

reality. Simulation with daylight using a sky model was studied by Mardaljevic [21] using *Radiance lighting simulation and rendering system* [38] and measured against real world illumination values for a single point on a floor of a simple model.

In 2001 Drago and Myszkowski [8] proposed a model for validation of global illumination algorithms based on the atrium at the University of Aizu in Japan. They carefully measured the geometry, surface reflectance for important surfaces, and luminaires including maintenance factors. The reference illumination values for 84 points were measured by a luxmeter. Furthermore, the rendered images were compared against the photographs in psychovisual experiment with 25 subjects. Schregle and Wienold [29] created an experimental setup based on a box similar to the box of Goral et al. [11]. It was equipped with sensors mounted to movable belts to allow for measuring illumination in different positions in the box.

3.2 Analytical and Representative Problem Test Scenes

Another approach was taken to test and validate global illumination algorithms by Smits and Jensen [31]. They proposed a set of six scenes aimed at typical accuracy problems occurring in global illumination computation. Similarly, Szirmay-Kalos et al. [33] designed a very simple scene (a sphere), where the illumination can be computed analytically. Although this is absolutely correct and elegant, the criticism for this is exactly the simplicity of the test geometry. Few experimental studies for small scale architectural scenes were performed, such as [35, 28, 26, 10] by the researchers in lighting by 2001, but the data for the test scenes are not publicly available.

The researchers from lighting research and technology, who were aware of severity of the validation the rendering software for purpose of lighting computation, prepared a validation standard CIE test suite [3]. This test suite consists of simple analytical and experimental scenes with known illumination in some predefined points. The design of test scenes is highly based on the previous work of Maamari [19, 20] including his PhD thesis [18]. The test suite required major effort for several years and it was launched to public in 2006. The simple case scenes in this test highlight a given aspect of lighting simulation to identify the source of possible errors. The conformity reports for preliminary or final version of the CIE tests were published for some rendered global illumination renderers [15, 14, 7]. Further, Mardaljevic [22] discussed different issues in carrying out meaningful validations of

lighting computation software.

4 Datasets in Computer Graphics

Algorithms in computer graphics have been tested using two major classes of datasets. The first one was prepared by researchers themselves. The second one was released by companies, for example from their production. Although there is no drive for benchmarking standardization for research practice, almost all the datasets used in research that were released to public prepared by anybody, became the de facto standard benchmarking datasets. This clearly shows that there is generally a lack of datasets for research.

In this chapter we discuss ordinary problems that researchers meet when they select the dataset for their research. Further, we list several publicly available datasets used in computer graphics with a focus on rendering. These are in fact all we are aware of to our best knowledge in December 2009.

4.1 Ordinary Problems with Datasets

Researchers have to consider a number of properties when selecting a dataset for an experiment. First goal is to objectively test and evaluate the proposed algorithm using the dataset as an input. The second goal is to avoid possible criticism from readers and reviewers for the dataset, which can be considered by them as:

- *small* and/or considered as *obsolete* and/or *overused* - each dataset is created at some time with some intention. It is natural that a dataset created 30 years ago does not fulfill the need on the complexity or accuracy imposed by the tested algorithms nowadays. As an example we can point to the well known Utah teapot [25], one of the first free-form models created. While this is a very nice dataset, it was created in 1975 and for most of the research carried out nowadays it is not sufficiently complex. Similarly, the folklore opinion is that many published global

illumination methods produce good results on the Cornell box [4], but they do not provide the satisfactory ones on other more complex scenes. It is still very useful to use Cornell box for initial testing of an algorithm implementation. However, a paper about global illumination is hardly to be accepted for publication if it uses only the Cornell box scene and scenes of similar complexity (as of year 2009).

- *visually unconvincing* or *unrealistic* - some datasets do not sufficiently or convincingly represent or resemble the real world that we assume to be the real subject of a research topic. We show two example dataset, Figure 4.1(a,b) for a visually unconvincing and Figure 4.1(c) for an unrealistic one. Let us further discuss the dataset as a result of some statistical model, such as that in Figure 4.1(a), taken from [32]. While the dataset can be sufficient to study a problem and have some interesting statistics properties useful to derive the complexity of an algorithm, the similarity between the dataset and the real world cannot be shown or proved. Simply put, the dataset appears to be visually unconvincing. In our experience [32] these datasets are difficult to be used in computer graphics with success (i.e., the acceptance of a paper with a new algorithm for publication).

- *insufficiently accurate* or *incomplete* - some datasets are nice and sufficiently complex, but they do not contain all the important properties required to carry out the computation. An example in predictive rendering is a large dataset of a building, for which we do not have measured/estimated luminaires or surface reflectance for a majority of surfaces. Or we do not have the real building to acquire reference photographs or the available reference photographs were taken for unknown daylight illumination, etc.

The hypothesis we would like to present is: *every digital dataset used for computer simulation of a real world for research such as computer graphics will once become obsolete.* This hypothesis is also valid for the dataset presented further in this paper. Basically, we can expect that the accuracy, i.e., the level of approximation of a real world behaviour, will at one moment become insufficient. Although this is rather a philosophical issue, the lifetime of datasets used in computer science experiments (and hence the utility of a research work that is documented, quantified, and validated by the experiments) is almost never considered.

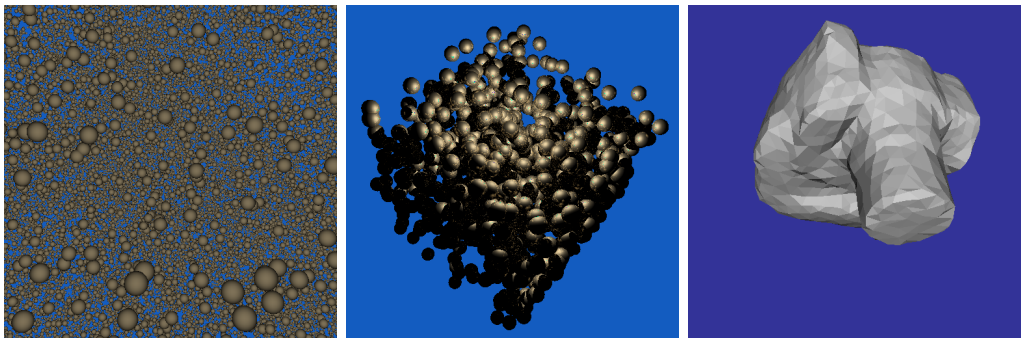

(a) (b) (c)

Figure 4.1: (a) and (b) Examples of visually unconvincing dataset (c) Example of unrealistic dataset (camera Kodak).

4.2 Architectural Datasets

Below we list several known datasets with the focus on those that can be used in the field of rendering and global illumination. There are only two datasets that are publicly available and have some reference images, geometry, reflectances, and luminaires. Therefore their description is complete for the purposes of validating predictive rendering algorithms:

- Cornell Box [4], with initial simple version by Goral et al. [11] in 1984 and completed by HDR photos in 2005,
  http://www.graphics.cornell.edu/online/box/
- Aizu Atrium [8], with 700,000 triangles, completed in 2005 by BTF data for 4 major surfaces by university of Bonn and HDR photographs taken in the environment in 2008,
  http://www.mpi-inf.mpg.de/resources/atrium/.

Other architectural datasets that were used and can be obtained for validation of global illumination algorithms are to our best knowledge incomplete, usually their corresponding real world counterpart is not available:

- Conference scene from the Radiance package [38] by Greg Ward, 1993, (no corresponding real world counterpart with reference images), (http://radsite.lbl.gov/radiance/
- Soda Hall model with roughly 1,500,000 triangles, prepared by Prof. Carlo Séquin, 1998 (no photographs under known daylight illumination, no description of light sources, and surface reflectances),
  http://coe.berkeley.edu/labnotes/0704/history.html

- Sponza Model by Marko Dobrovic, 2002, (no corresponding counterparts or reference images),
  http://hdri.cgtechniques.com/~sponza/

- Sibenik Cathedral Model by Marko Dobrovic, 2001, and other two scenes (BLOCHI's scene and POSTSPARKASSE), less frequently used, no corresponding counterparts or reference images,
  http://hdri.cgtechniques.com/~sibenik2/index_sibenik.htm

- Power Plant Model by Walkthru Group at University of North Carolina, prepared in 1998 and released later to public, with about 13 million triangles (no light sources, no real world counterpart),
  http://gamma.cs.unc.edu/POWERPLANT/

Other public repositories of geometric objects/scenes used in computer graphics available on the Internet in general by December 2009 are to our best knowledge:

- Standard Procedural Benchmark (SPD) dataset [13], prepared by Eric Haines in 1987, for benchmarking ray tracing algorithms,
  http://www.acm.org/tog/resources/SPD/,

- Stanford 3D repository of digitized objects, released in 1996,
  http://graphics.stanford.edu/data/3Dscanrep/,

- AIMSHAPE collection of objects as a result of EU IST project, version 4.0, March 2007,
  http://shapes.aim-at-shape.net/,

- BES scene collection of objects downloaded from the web, initiated by Vlastimil Havran, 2001,
  http://dcgi.felk.cvut.cz/BES/scenes/www/,

- BART scenes by Lext et al. [17], 3 animated scenes for benchmarking animated ray tracing methods, 2001,
  http://www.ce.chalmers.se/research/group/graphics/BART/,

- The Utah 3D Animation Repository that has nine key-framed animated scenes, initiated by Ingo Wald, 2006,
  http://www.sci.utah.edu/~wald/animrep/

- Animated meshes by Robert W. Sumner and Jovan Popovic, 2004,
  http://people.csail.mit.edu/sumner/research/deftransfer/data.html

- Animated figures by Daniel Vlasic, 2008,
  http://people.csail.mit.edu/drdaniel/

Interestingly, the number of scenes used for experiments in scientific papers is by orders of magnitude smaller than the number of papers published, at least in the field of computer graphics.

Let us mention other possibilities for acquiring geometric datasets. There are commercially available datasets including usually individual objects in formats of commercial packages, but since they cannot be used by independent researchers for free and their format is often proprietary, these datasets are almost as difficult to use as the datasets of private companies in a research project. In addition, the dataset properties are not known in advance and the characteristics of a dataset can be reviewed only after buying them.

In addition, there is a number of free available 3D models at Internet websites such as http://archive3d.net, usually containing individual objects created by independent artists. Unfortunately, these are usually stored in proprietary formats of commercial or free packages (such as povray, http://www.povray.org/) that also suffer from the problem of data migration and the lack of standard and widespread formats. The conversion can be be long and tedious, as usually there is no existing real world counterpart and/or the accuracy of the model is quite limited with respect to reality. In addition, the availability of these datasets on the web is typically rather short or unknown and the use of dataset often requires a prior consent of its author. All these problems together usually severely limit the use of these datasets in research practice.

5 The MPI Informatics Building Model

In this chapter we introduce the MPI Informatics building model. The motivation to prepare this dataset was solely to alleviate the lack of architectural models useful for global illumination algorithms and lighting research. The idea of the project has been to prepare a sufficiently complex dataset that allows for simulation of subtle and complex illumination effects. In addition, it was required to have its physical counterpart well accessible and available in Europe to allow for possible additional acquisition of (reference) data from the real world environment. As we have discussed already, this data (such as photographs) is needed to validate the algorithms in predictive image synthesis. In addition to obvious affiliation of the authors at the time the project started, the choice felt on the building of Max-Planck-Institut für Informatik, as it has all the required properties and it poses a nice large square-like atrium open space, which provides nice interior views from many perspectives. The computation of light transport was estimated to be considerably and sufficiently complex as the number of light sources contributing to the interior of the building's atrium is high (see Figure 1.1).

The real building of the MPII was built between Summer 1993 and Autumn 1995, the outside photograph of the building is in Figure 5.1(a). The initial work on the virtual reconstruction started in September 2003 as a part of the RealReflect IST project in the Frame Programme Six supported by the European Union.

A simple digital model of the building existed, created by architects before the building was built in year 1993, with known visualization as shown in Figure 5.1(b). However, this data was of little use as severe problems has arisen with the data migration. The data in DXF format from 1993 as imported to commercial 3D modeling software in September 2003 were neither correct nor complete nor sufficiently complex, see Figure 5.2(a) and (b).

Below we describe the created dataset in four parts that are substantial

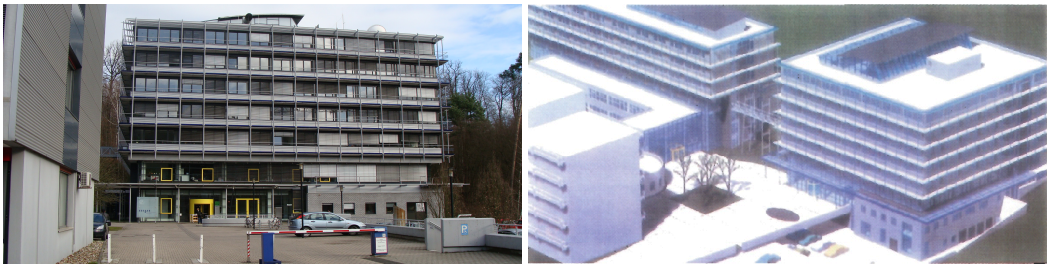

(a) (b)

Figure 5.1: (a) Photograph of a real building from outside, (b) visualization of the building by architects, 1993.

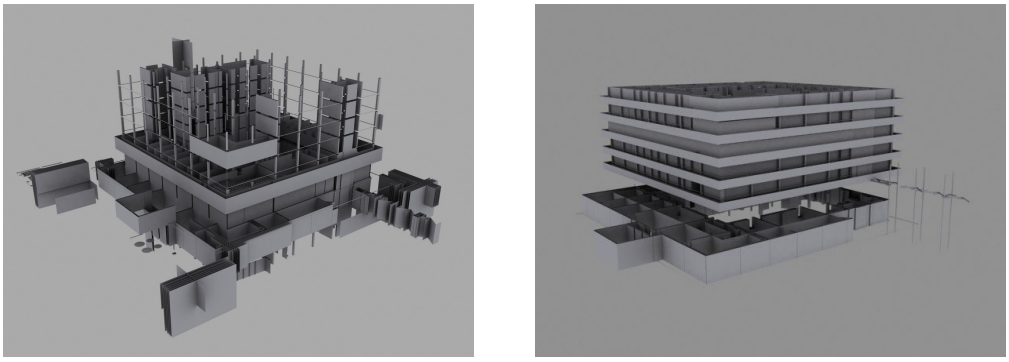

(a) (b)

Figure 5.2: Starting work on the old data in September 2003 (a) data migration problem, visualization of import data from architects in DXF format, (b) the same dataset after manual repositioning.

for validation in predictive image synthesis, namely the geometry, luminaires, surface reflectances, and taken HDR photographs.

5.1 Geometry

The initial geometry of the MPI Informatics building model was created by manually repositioning the imported DXF data produced by architects in 1993, followed by a careful check against the real building and architectural plans (blueprints in A1 format, scale 1:100). The modeling process took majority of time from the whole project and it was laborious and time consuming. The level of detail to which the geometry was selected for reconstruction, includes such parts of the building that are fixed in the building, are not supposed to change with time or are visually important with respect to reference photographs (Chapter 5.2). Therefore, in addition to obvious parts of the building such as main concrete construction, doors, windows, window shutters, heating, ventilation, luminaires geometry, roof, outer metal plates, stairs and metal and glass fences, the MPI Informatics building model also includes furniture and plants in the atrium of the building. It was necessary to carry out geometric modeling in layers due to the limited memory and performance of modeling software for the hardware used, in particularly in year 2003.

The decomposition of geometry into 35 layers in the resulting dataset allows us to simplify the dataset when needed, for example, by removing the furniture in offices from the whole building or only from some floors. This is particularly advantageous with the two-level organization of the data in files we used; there is one main file and several files that are included in the main file. Hence the simplification by removing the furniture corresponds only to commenting out 21 lines in the main file. The decomposition into the layers is thus useful for simple manipulation with the dataset.

There are many repeated parts in the model that allowed for reusing some of the modeled geometry. This includes for example the windows, doors, and the furniture in offices. The difficulty was in the verification of equivalence of the geometry and the necessity to correct positioning of the reused geometry in space to correspond to reality. These tasks frequently required measuring the positions and sizes of the geometry in the building.

The whole model consists of roughly 73 million of triangles of different sizes, without the furniture in offices it is 23 million of triangles. The ratio of the sizes between the largest and the smallest triangle is more than 4 orders of magnitude - the small geometric details are finely tessellated, while for example the triangles for walls or railing span over several meters.

Moreover, the triangles can be of a different shape, starting from those with equal-sized edges to a very elongated ones (two sides by orders of magnitude larger than the third size of a triangle), e.g. the cylindrical parts of railing around the atrium. To conclude, the geometry of the building can be considered moderately to highly complex (as of year 2009). After the export from commercial modeling software to VRML 97 [39] the final geometry consists of only triangles; no higher-order primitives are present.

5.2 Reference HDR photos

Eight HDR reference photographs inside the building were taken in the night of June 2004 to avoid the outdoor illumination of unknown daylight condition. The nearby outdoor artificial illumination was negligible. The pictures were taken as 15 shots with different exposure for each image, using Kodak Professional DCS560 camera with Lenses EF 14mm. The camera was controlled by a computer program and the resulting HDR images were put together using Robertson et al. algorithm [30]. Two pairs of these images were taken at the same position of the camera, but the lighting condition were changed. The lighting conditions inside the building for the moment of taking photographs were carefully recorded by the list of switched on luminaires. All the doors including those to offices were closed in the whole building, so the lack of luminaires in offices does not bring an obstacle to comparing the reference photographs to the images obtained by computer simulation.

The position and orientation of the camera for taking photographs was also recorded and later in the final model further iterated to get more accurate estimate of cameras in an interactive ray tracing application based on the visual match of a geometry with the photographs.

The tonemapped images from HDR photographs with a short description of viewpoints are given in Appendix A.

5.3 Luminaires

There are seven types of luminaire used in the building, where for all of them their underlying geometry was modeled. Total number of luminaires in the MPI Informatics building model is 623, which excludes the emergency luminaires and the luminaires located in the offices. The light emission from luminaires was approximated by far-field photometry for six types of luminaires. This means that each luminaire is simplified to a point and we represent the

directional dependence of radiance from this point. This is often referred to as a goniometric diagram [37]. As there are no available data from luminaire producers, the goniometric diagrams had to be measured. The measured data were converted to IESNA-95 format [1] (type C).

As the number of luminaires was large and there was no suitable and sufficiently accurate measurement gantry such as high dynamic range luxmeter, so called maintenance factors for all installed luminaires were not measured. The maintenance factor with nominal value 100% describes the decrease of luminaire intensity due to the ageing of the light source in the luminaire, accumulation of dust on the cover, etc. To allow for successful lighting simulation the point that represents the center of goniometric diagram was positioned about ten millimeters in front of the geometry of the luminaire. This appeared as necessary to avoid self-occlusion in the simulation software that would be caused by the geometry of the luminaires themselves, when computing the direct illumination. The emission from the emergency light sources was not possible to measure; the free samples/spare parts of this luminaire were not available and this luminaire type has several variants with different arrows on the plate, which also affects the goniometric diagram. However, the geometry of these luminaires was created and positioned in the dataset of MPI Informatics building model.

The detailed description of luminaires including their measured characteristics is given in Appendix B.

5.4 Surface Reflectances

The number of different materials covering the created geometry identified in the building as important for the visual appearance was relatively high - fifty-two different materials. There were several major obstacles that prevented us to measure the bidirectional-reflectance distribution function (BRDF) for these materials, that could be necessary to complete the reference data for this dataset. First, it was impossible to obtain the planar samples for these materials. For ready to use BRDF acquisition methods and commercial solutions it is necessary to provide these samples. However, there were no free planar samples of the materials and it was not allowed or possible to extract them from the building.

For all the reasons above, the BRDF was only estimated with the help of reflectance database project CUReT (Columbia-Utrecht Reflectance and Texture Database) [6] that describes 61 materials in Oren-Nayar reflectance model. This is fortunately one of the formats used in the scene format of Physically based rendering toolkit (PBRT) [27], to which we converted

data as well. The colours of the materials were manually corrected to fit to acquired photographs from the real environment. This estimation of BRDF is an obvious source of inaccuracies in the whole MPI Informatics building model, but there was no other option at the course of the project run.

The assignment and the definition of surfaces with photographs of representative parts is given in Appendix C.

5.5 Additional Data

Several additional data were acquired from the building to support the reconstruction and to document the status of the building. This includes a set of photographs from the interior of the building and from the outside and three short low quality videos to give an impression about the building's architecture.

5.6 Dataset Organization and Conversion

The modeled data were converted in custom based conversion software, prepared particularly for this project. The design choices for this software with GUI based on wxWidgets and its implementation are described in detail in the Master Thesis of Jiří Drahokoupil [9]. The overall data conversion flow can be described as follows. First, the data were exported from 3D commercial modeling software to open standard format, VRML 97. The textual datasets were created for measured luminaires and estimated reflectances. It was necessary to provide the correspondence between data in the commercial modeling software and the final model. For this purpose a special naming convention was used already in the 3D commercial modeling software from the whole beginning of the project to make a correspondence between goniometric diagrams in IESNA-95 format and the resulting geometry. The second way to provide the correspondence is the diffuse color of the materials in 3D commercial modeling software. The materials were uniquely and consistently assigned during the modeling. The color of the geometry after export was then used as a key to assign the surface reflectances correctly.

The input data (geometry, reflectances, luminaire data) were imported to the custom based software and exported to format of the PBRT software [27] and to the extension of the VRML 97 standard [39] to allow the definition of luminaires by IESNA-95 format. This extension is as follows:

```
PROTO GonioLight [
   exposedField MFString url []
```

```
   exposedField SFVec3f location 0 0 0
   exposedField SFVec3f direction 0 0 -1
   exposedField SFVec3f baseVector 1 0 0
   exposedField SFColor color 1 1 1
   exposedField SFFloat intensity 1
   exposedField SFBool on TRUE
] { }
```

6 Discussion

In this chapter we want to discuss the properties of the MPI Informatics building model, including the limitations of the dataset and unexpected problems we have met during the course of the project.

6.1 Limitations and Accuracy

The created model cannot completely reflect the reality accurately, it is only approximating it to some level of detail. This is however expected for reconstruction of all complex real world data. Let us discuss the sources and reasons for these inaccuracies. There are some missing parts of the reality that were not modeled for one of the following reasons:

- the geometry was not relevant for the assumed simulation with respect to reference photographs,
- the geometry was very unique and/or inaccessible for measurements,
- the geometry was assumed to be frequently changing,
- the geometry was so detailed that there was not enough time to model this level of detail.

We list these missing parts without the claim of the list's completeness: parking lot and sky-walk to CS building, equipment in the underground floor (Building Administration Department), showers, equipment and furniture on the ground floor for the administration department (rooms 002-017), phones and defibrillator, equipment and furniture in rooms 016-023, furniture on the south and east 1st floor (today Information Services & Technology and IMPRS), coffee machine and cups on the first floor, service ladder below the roof on the 6th floor, luminaires in offices, emergency luminaires (i.e. goniometric diagrams, geometry of the luminaires is finished), kitchens and their

equipment, toilets, printer rooms, cleaning rooms, storage rooms, the art installation Klang-und Licht Installation by Peter Vogel, small art exhibitions in the building, photographs and other image materials on boards, the furniture and other equipment in offices of group directors and their secretaries, computers and their accessories anywhere (as they were changing too often).

However, even without these many details the MPI Informatics building model is quite complex and sufficient to allow the validation of synthesized images against the reference photographs, at least for subjective evaluation of rendered images and reference HDR photographs.

6.2 Problems

In the scope of the project we have encountered several problems caused by our own wrong assumptions that we want to report for the benefit of similar projects in future.

First, our expectation to reuse only ten years old data made by architects was overly optimistic. The problem known as data migration and data completeness was severe for the data we obtained. Second, the expectation that the export to ISO standard (VRML 97) from a commercial software will be working correctly was also not met. In particular, the model parts that were modeled by negative scaling (such as doors) did not export to correct positions, although their position was correct in the commercial software. Third, the expectation that the commercial software will be backward compatible between two of its releases for its own proprietary format was also wrong. It caused additional work and possibly the geometric bugs that are still present in the model geometry, although we tried to correct them and spent much time on this unexpected problem. Fourth, our expectation that we will be able to get samples of materials and measure the BRDF for those simply failed. Fifth, we did not expect a problem in the PBRT software that caused it to crash when many samples for a pixel were used in the rendering images. For this reason the final test images presented with the model on website are of limited quality. Sixth, the accuracy of modeling living plants is principally limited and we opted rather for rough approximation by using procedurally generated trees of similar shape and visual impression. Last but not least, the problem was that even during relatively small period of time in the beginning of the project the building and its accessories were changed. In our opinion and experience it is quite difficult to keep the pace of the digital model with the populated building, maintained by building administration.

Even if there were many problems, we believe according to the achieved

results, i.e., the preliminary rendered images and their subjective comparison with the real world photographs from the building, that the MPI Informatics building model is and will be useful in future. We hope that some of the problems and limitations listed above will be possible to correct in the future release of the dataset.

7 Conclusion and Future Work

In this report we have described some problems with geometric datasets, in particular architectural ones in the scope of computer graphics and lighting research. We described how this relates to the reproducibility of a research work. Having published a research paper, its experimental results can be reproduced only for the same datasets. To allow for a real reproducibility of the results (that are essential and inseparable part of published papers) only publicly available datasets (or those that can be later surely released public) should be used. Further, we discussed typical problems with the datasets and the criteria that have to be considered by a researcher upon selection of a dataset for testing and evaluation of his/her work. We described the current state of the art in availability of these datasets and surveyed the most important related work in predictive image synthesis in the field of computer graphics and lighting research.

We have described our effort to create *the MPI Informatics building model* for the real building of Max-Planck-Institut für Informatik in Saarbrücken and the modeling choices and problems we had to solve. The MPI Informatics building model consists of geometry, luminaires, estimated surface reflectances, reference HDR photographs, and additional data. We carried out preliminary rendering of images from the MPI Informatics building model in PBRT software. It shows subjectively good visual match between the model and the reference photographs. We discussed the dataset limitation and problems encountered.

In addition to obvious use of the MPI Informatics building model in experimental research projects in various communities there is some possible future work on the dataset itself. One task is to correct the geometric inaccuracies and errors in the dataset and possibly to complete it by other now missing, but relatively important parts. Another appealing task that could extend the applicability of the dataset in research is to modify the current conversion software to allow for dynamization of movable parts of the build-

ing, such as doors, windows, and window shutters, that with could provide much higher variability of data according to user's choice. To enhance further the complexity the luminaires and their geometry in the offices can be positioned. Obviously, another important task is to complete the model by acquisition of BRDF or BTF data for all or at least the majority of surface materials used in the model. It is also required to measure far-field photometry for emergency luminaires and position the luminaires in the offices. It would also be nice to provide near-field photometry for the luminaires in the building as due to the length of some type of luminaires the far-field photometry assumption is not valid.

Future releases of the dataset for MPI Informatics building model, with possible extensions and correction of datasets will become available at URL:

http://www.mpi-inf.mpg.de/resources/mpimodel/

Acknowledgements

We would like to thank several people and institutions for their help during the work on the project of the MPI Informatics building model and also the funding resources. We can list only those that were most important for our project:

- Karol Myszkowski for his kind help and advices before and during the project. We were highly inspired by his and Frederic Drago Atrium project for predictive rendering. Without his help and support our project would be hardly possible.

- Roxane Wetzel from MPII administration and Prof. Dr. Wolfgang Paul from the University of Saarbrücken, who helped us to get some of the original building 3D data (in DXF format) to start the project in 2003. Further again to Roxane Wetzel for supplying us with the drawings from the architects of the real MPII building and for the frequently and kindly helping us in the whole lifetime of this project.

- Akiko Yoshida, Grzegorz Krawczyk, and Rafal Mantiuk for helping us with the HDR image acquisition, measurement preparation, and post-processing in June 2004.

- European Union within the scope of RealReflect IST project (IST-2001-34744) for partial funding of the project from June 2003 until November 2004. The project of MPI Informatics building model was initially motivated by the needs and objectives of the RealReflect project. Further, this work has been partially funded by the Ministry of Education, Youth and Sports of the Czech Republic under the research program MSM 6840770014 and LC-06008 (Center for Computer Graphics), and the Aktion Kontakt OE/CZ grant no. 2009/6.

- Prof. Jiří Habel and Dipl.-Ing. Marek Bálský from the Czech Technical University in Prague, Faculty of Electrical Engineering, Department of

Electrical Power Engineering, for their kind help and advices with the measurement of luminaires.

- The administration of MPII building and of computer graphics group, in particularly to Sabine Budde, Conny Liegl, Michael Bentz, and Gabi Holzer for really efficient and responsive administrative help in our project. We also thank Michael Laise and Axel Koeppel in the building administration for the access to several spare parts needed for the data acquisition. Further we would like to thank the computer services and technology department at MPII for providing us all the hardware and software support needed by this project, in particularly Uwe Brahm.

- Michal Hapala for kindly proofreading the manuscript.

- Many colleagues and friends at MPII for sharing their time and interests in Saarbrücken, providing us with the moral support and encouragement, and for having fun with during our stay at MPII.

Bibliography

[1] I. Ashdown. Thinking Photometrically Part II. In *LIGHTFAIR 2001 Pre-Conference Workshop*, pages 1–46, Mar. 2001.

[2] W. L. Carroll. Daylighting simulation: methods, algorithms, and resources - A Report of IEA SH Task 21/ ECBCS ANNEX 29. Technical report, Lawrence Berkeley National Laboratory:, Dec. 1999.

[3] CIE 171:2006. Test Cases to Assess the Accuracy of Lighting Computer Programs, 2006.

[4] M. F. Cohen and D. P. Greenberg. The Cornell Box, 1985. http://www.graphics.cornell.edu/online/box/.

[5] M. F. Cohen and D. P. Greenberg. The hemi-cube: a radiosity solution for complex environments. In *SIGGRAPH '85: Proceedings of the 12th annual conference on Computer graphics and interactive techniques*, pages 31–40, New York, NY, USA, 1985. ACM.

[6] K. Dana, B. Van-Ginneken, S. Nayar, and J. Koenderink. Reflectance and Texture of Real World Surfaces. *ACM Transactions on Graphics (TOG)*, 18(1):1–34, Jan 1999.

[7] Dau Design and Consulting Inc. Validation of AGi32 against CIE 171:2006, June 2007.

[8] F. Drago and K. Myszkowski. Validation proposal for global illumination and rendering techniques. *Computers & Graphics*, 25(3):511–518, 2001.

[9] J. Drahokoupil. Predictive rendering of the MPII building. Master's thesis, CTU–FEE, Department of Computer Science and Engineering, Prague, Czech Republic, Feb 2009. (supervised by Vlastimil Havran, in Czech language).

[10] H. Eissa and A. Mahdavi. On the Potential of Computationally Rendered Scenes for Lighting Quality Evaluation. In *Seventh International IBPSA Conference*, pages 797–804, 2001.

[11] C. M. Goral, K. E. Torrance, D. P. Greenberg, and B. Battaile. Modeling the interaction of light between diffuse surfaces. In *SIGGRAPH '84: Proceedings of the 11th annual conference on Computer graphics and interactive techniques*, pages 213–222, New York, NY, USA, 1984. ACM.

[12] D. P. Greenberg, K. E. Torrance, P. Shirley, J. Arvo, E. Lafortune, J. A. Ferwerda, B. Walter, B. Trumbore, S. Pattanaik, and S.-C. Foo. A framework for realistic image synthesis. In *SIGGRAPH '97: Proceedings of the 24th annual conference on Computer graphics and interactive techniques*, pages 477–494, New York, NY, USA, 1997. ACM Press/Addison-Wesley Publishing Co.

[13] E. Haines. A proposal for standard graphics environments. *IEEE Comput. Graph. Appl.*, 7(11):3–5, 1987.

[14] V. Havran, K. Myszkowski, J. Wurster, and C. Soler. D10.3: Report on Light Simulation in Architecture, Sept. 2005.

[15] Integra Inc. Results of CIE TC.3.33 Tests for Inspirer, 2004.

[16] K. Karner and M. Prantl. A Concept for Evaluating the Accuracy of Computer Generated Images. In *Proceedings of Spring Conference on Computer Graphics 1996*, pages 145–154, 1996.

[17] J. Lext, U. Assarsson, and T. Möller. A Benchmark for Animated Ray Tracing. *IEEE Comput. Graph. Appl.*, 21(2):22–31, 2001.

[18] F. Maamari. *Lighting simulation, limits and potentials.* PhD thesis, INSA de Lyon, 2003.

[19] F. Maamari and M. Fontoynont. Analytical tests for investigating the accuracy of lighting programs. *Lighting Res. Technology*, 35:225–242, 2003.

[20] F. Maamari, M. Fontoynont, M. Hirita, J. Koster, C. Marty, and A. Transgrassoulis. Reliable Datasets for Lighting Programs Validation, Benchmark Results. In *Excerpt from the Proceedings of CISBAT 2003*, pages 241–246, 2003.

[21] J. Mardaljevic. *Daylight Simulation: Validation, Sky Models and Daylight Coefficients.* PhD thesis, De Montfort University, 2000.

[22] J. Mardaljevic. Verification of program accuracy for illuminance modelling: assumptions, methodology and an examination of conflicting findings. *Lighting Research and Technology*, 36(3):217–239, 2004.

[23] Max-Planck-Society. Rules of Good Scientific Practice, November 2000. http://www.mpg.de/pdf/procedures/rulesScientificPract.pdf.

[24] G. W. Meyer, H. E. Rushmeier, M. F. Cohen, D. P. Greenberg, and K. E. Torrance. An experimental evaluation of computer graphics imagery. *ACM Trans. Graph.*, 5(1):30–50, 1986.

[25] M. Newell. Utah Teapot, 1975. http://en.wikipedia.org/wiki/Utah_teapot.

[26] A. Pellegrino and L. Caneparo. Lighting Simulation for Architectural Design: a Case Study, 2001.

[27] M. Pharr and G. Humphreys. *Physically Based Rendering: From Theory to Implementation*. Morgan Kaufmann Publishers Inc., San Francisco, CA, USA, 2004. http://www.pbrt.org.

[28] G. G. Roy. A Comparative Study of Lighting Simulation Packages Suitable for use in Architectural Design, 2000. Perth: Murdoch University, School of Engineering.

[29] R. Schregle and J. Wienold. Physical Validation of Global Illumination Methods: Measurement and Error Analysis. *Comput. Graph. Forum*, 23(4):761–781, 2004.

[30] M. R. Sean, M. A. Robertson, S. Borman, and R. L. Stevenson. Dynamic Range Improvement Through Multiple Exposures. In *In Proc. of the Int. Conf. on Image Processing (ICIP'99)*, pages 159–163. IEEE, 1999.

[31] B. Smits and H. W. Jensen. Global Illumination Test Scenes. Technical Report UUCS-00-013, Computer Science Department, University of Utah, June 2000.

[32] L. Szirmay-Kalos, V. Havran, B. Balázs, and L. Szécsi. On the Efficiency of Ray-shooting Acceleration Schemes. In A. Chalmers, editor, *Proceedings of the 18th Spring Conference on Computer Graphics (SCCG 2002)*, pages 89–98, Budmerice, Slovakia, 2002. ACM Siggraph.

[33] L. Szirmay-Kalos, L. Kovács, and A. M. Abbas. Testing Monte-Carlo Global Illumination Methods with Analytically Computable Scenes. In *WSCG*, pages 419–426, 2001.

[34] A. Takagi, H. Takaoka, T. Oshima, and Y. Ogata. Accurate rendering technique based on colorimetric conception. *SIGGRAPH Comput. Graph.*, 24(4):263–272, 1990.

[35] M. S. Ubbelohde and C. Humann. Comparative Evaluation of Four Daylighting Software Programs. In *Proceedings of the 1998 Summer Study on Energy Efficiency in Buildings, ACEEE*, pages 325–340, 1998.

[36] C. Ulbricht, A. Wilkie, and W. Purgathofer. Verification of Physically Based Rendering Algorithms. *Computer Graphics Forum*, 25(2):237–255, June 2006.

[37] C. Verbeck and D. Greenberg. A Comprehensive Light-Source Description for Computer Graphics. *IEEE Comput. Graph. Appl.*, 4(7):66–75, 1984.

[38] G. J. Ward. The RADIANCE lighting simulation and rendering system. In *SIGGRAPH '94: Proceedings of the 21st annual conference on Computer graphics and interactive techniques*, pages 459–472, New York, NY, USA, 1994. ACM.

[39] Web3D consortium. ISO/IEC 14772-1:1997 Virtual Reality Modeling Language (VRML), 1997. http://www.web3d.org/x3d/specifications/vrml/.

[40] Wikipedia. Reproducibility, 2009. http://en.wikipedia.org/wiki/Reproducibility.

8 Appendix A - Reference Photographs

In this appendix we provide the pictures of eight reference photographs from the real building as they were capture and tonemapped for printing.

Figure 8.1: Viewpoint 1 - the 2nd floor.

Figure 8.2: Viewpoint 2 - the 2nd floor.

Figure 8.3: Viewpoint 3 - the 2nd floor.

Figure 8.4: Viewpoint 4 - the 2nd floor.

Figure 8.5: Viewpoint 5 - the 5th floor.

Figure 8.6: Viewpoint 6 - the 4th floor.

Figure 8.7: Viewpoint 7 - the 4th floor.

Figure 8.8: Viewpoint 8 - the 6th floor.

9 Appendix B - Luminaires

In this appendix we describe the luminaires used in the virtual reconstruction of MPII building and the process of these data acquisition and conversion.

Luminaire # 1

Basic Parameters

Type:	Louis Poulsen 94-02511	
Properties:	Shield Length:	160 mm
	Light shield outer diameter:	50 mm
	Light shield inner diameter:	45 mm
	Light shield glass thickness:	5 mm
	Lamp socket outer diameter:	82 mm
	Lamp socket inner diameter:	62 mm
	Luminous intensity	106.23 $[lumen \cdot m^{-2}]$
	Chromaticity temperature:	4100 [K]

Bulb properties

Type: Radium Ralux RX-D/E 13W/840.

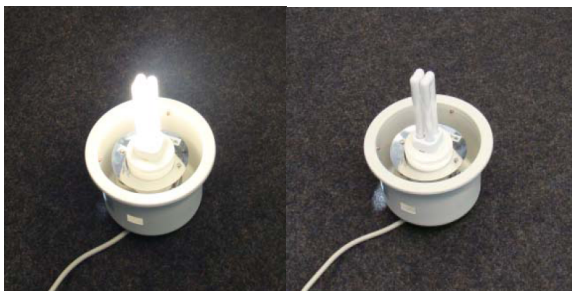

Figure 9.1: Luminaire #1 without light shield switched on and off.

Figure 9.2: Lamp socket for Louis Poulsen luminaire (1).

Figure 9.3: Lamp socket for Louis Poulsen luminaire (2).

IESNA LM63-1995 description

```
IESNA:LM-63-1995
[TEST] CTU Prague, FEL Katedra elektroenergetiky
[MANUFAC] Louis Poulsen
[LUMCAT] Louis Poulsen 94-02511
[LUMINAIRE] Wall lamp with cylindrical lampshade(shutter)
[LAMP] Radium Ralux RX-D/E 13W/840
[DATE] 3.6.2008, Ing.Marek Balsky, Bc.Jiri Drahokoupil
[OTHER]
TILT=NONE
1 900 1 37 1 1 2 -0.165 0 0.165
1.0 1.0 13.0
0 5 10 15 20 25 30 35 40 45 50 55 60 65 70 75 80 85 90 95 100 105 110
115 120 125 130 135 140 145 150 155 160 165 170 175 180
0
122.4 125.6 134 128 126.8 126 125.2 122 115.2 106.4 96.8 86.8 77.2
70.4 64.8 59.2 54.8 50.8 49.2 47.6 45.76 43.36 40.76 38.8 36.68
34.52 32.36 30.2 28.04 25.88 23.72 21.56 19.4 17.24 12.01 10.87 8.27
```

Luminaire diagrams

As the luminaire has highly symmetric light radiation, the measurement for goniometric diagram was taken only for one set of angles in θ direction for range of angles (0°–180°).

Figure 9.4: Bulb Radium Ralux RX-D/E

Figure 9.5: The 3D model of luminaire #1 (Luous Poulsen) with light shield.

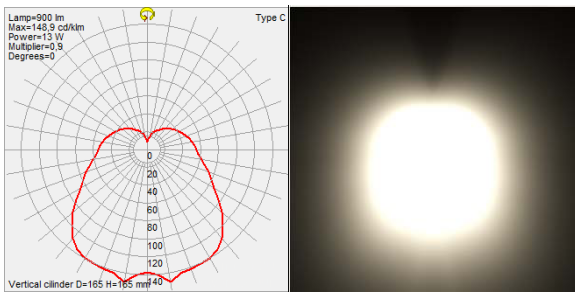

Figure 9.6: Luminaire exitance diagram and the rendered image for this description for luminaire #1 (Louis Poulsen).

Luminaire # 2

Basic Parameters

Type:	Siemens 5LJ180 7-1CD2 EVG	
Properties:	Length:	1230 mm
	Width:	46 mm
	Height(with cage):	85 mm
	Height(without cage):	50 mm
	Luminous intensity:	5.11 $[lumen \cdot m^{-2}]$
	Chromaticity temperature:	4000 [K]

Fluorescent Tube

Type: Radium NL 36W/840 Spectralux Plus Cool White

Figure 9.7: Luminaire holder # 2.

Figure 9.8: Fluorescent tube for luminaire # 2.

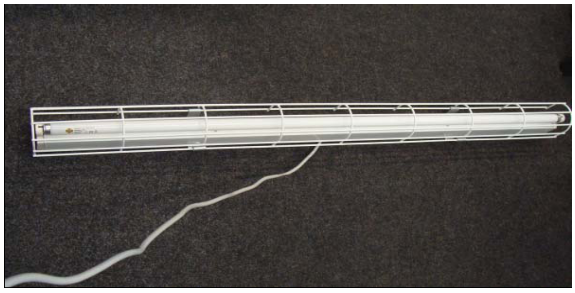

Figure 9.9: Luminaire #2 without light shield switched off.

Figure 9.10: Luminaire #2 without light shield switched on.

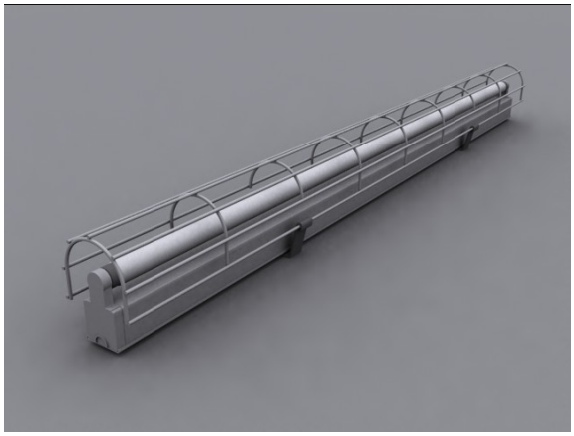

Figure 9.11: The 3D Model of luminaire # 2.

IESNA LM63-1995 description

```
IESNA:LM-63-1995
[TEST] 24909, SITECO
[MANUFAC] Siemens
[LUMCAT] Siemens 5LJ180 7-1CD2 EVG
[LUMINAIRE] freistrahlend
[LAMP] Radium NL 36W/840 Spectralux Plus Cool White
[DATE] 3.6.2008, Bc.Jiri Drahokoupil
[OTHER] SOURCE EULUMDAT file: siteco.ldt
TILT=NONE
1 3350.0 3.350 37 7 1 2 1.18 0.05 0.00
1.0 1 0.0
0.0 5.0 10.0 15.0 20.0 25.0 30.0 35.0 40.0 45.0 50.0 55.0 60.0 65.0 70.0 75.0 80.0
 85.0 90.0 95.0 100.0 105.0 110.0 115.0 120.0 125.0 130.0 135.0 140.0 145.0 150.0
 155.0 160.0 165.0 170.0 175.0 180.0
0.0 15.0 30.0 45.0 60.0 75.0 90.0
128.0 128.0 129.0 130.0 131.0 134.0 137.0 140.0 143.0 144.0 145.0 145.0 144.0 142.0
 139.0 133.0 126.0 120.0 118.0 118.0 118.0 119.0 119.0 109.0 95.0 81.0 66.0 51.0
 37.0 24.0 11.0 1.0 0.0 0.0 0.0 0.0 0.0
128.0 128.0 128.0 128.0 128.0 129.0 130.0 130.0 130.0 130.0 129.0 128.0 125.0 122.0
 118.0 112.0 104.0 97.0 94.0 94.0 96.0 96.0 93.0 83.0 71.0 59.0 47.0 35.0 24.0 15.0
 6.0 1.0 0.0 0.0 0.0 0.0 0.0
128.0 128.0 128.0 127.0 125.0 124.0 122.0 120.0 118.0 116.0 114.0 110.0 107.0 102.0
 97.0 90.0 82.0 74.0 71.0 71.0 73.0 72.0 67.0 58.0 47.0 38.0 28.0 19.0 12.0 6.0 2.0
 0.0 0.0 0.0 0.0 0.0 0.0
128.0 128.0 128.0 127.0 125.0 124.0 122.0 120.0 118.0 116.0 113.0 110.0 106.0 102.0
 96.0 90.0 82.0 74.0 70.0 71.0 73.0 72.0 67.0 57.0 47.0 37.0 28.0 19.0 12.0 6.0 2.0
 0.0 0.0 0.0 0.0 0.0 0.0
128.0 128.0 128.0 127.0 125.0 124.0 122.0 120.0 118.0 116.0 113.0 110.0 106.0 102.0
 96.0 90.0 82.0 74.0 70.0 71.0 73.0 71.0 66.0 57.0 47.0 37.0 28.0 18.0 12.0 7.0 2.0
 0.0 0.0 0.0 0.0 0.0 0.0
128.0 127.0 126.0 124.0 121.0 117.0 113.0 109.0 103.0 98.0 92.0 85.0 78.0 70.0 62.0
 54.0 45.0 38.0 35.0 35.0 36.0 36.0 33.0 29.0 24.0 19.0 14.0 9.0 6.0 3.0 1.0 0.0 0.0
 0.0 0.0 0.0 0.0
128.0 126.0 124.0 121.0 117.0 111.0 105.0 97.0 89.0 80.0 70.0 60.0 49.0 39.0 28.0
 18.0 8.0 2.0 0.0 0.0 0.0 0.0 0.0 0.0 0.0 0.0 0.0 0.0 0.0 0.0 0.0 0.0 0.0 0.0 0.0
 0.0 0.0
```

Luminaire diagrams

The measurement has been take for horizontal planes at angles 0°, 15°, 30°, 45°, 60°, 75°, and 90°.

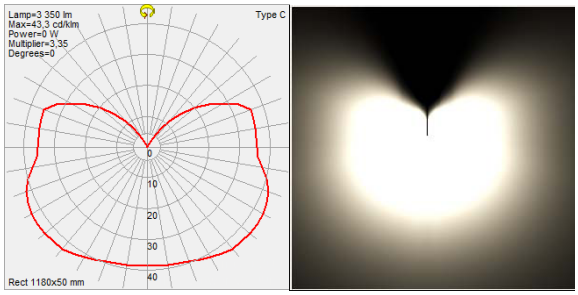

Figure 9.12: Luminaire radiant exitance diagram and the rendered image for this description for luminaire #2 for horizontal plane at angle 0°.

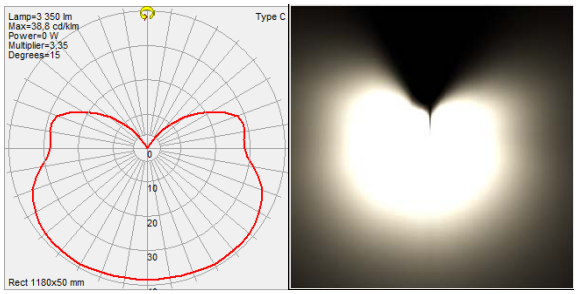

Figure 9.13: Luminaire exitance diagram and the rendered image for this description for luminaire #2 for horizontal plane at angle 15°.

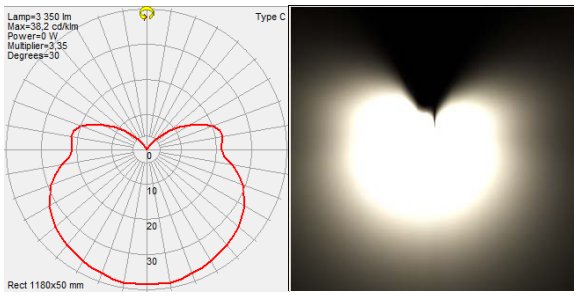

Figure 9.14: Luminaire exitance diagram and the rendered image for this description for luminaire #2 for horizontal plane at angle 30°.

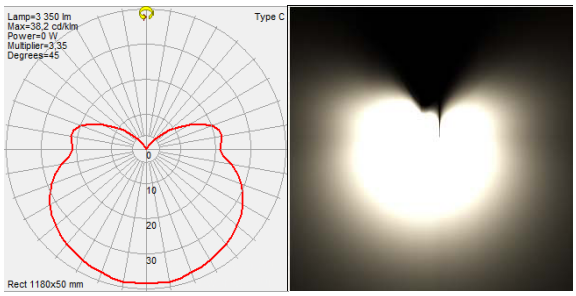

Figure 9.15: Luminaire exitance diagram and the rendered image for this description for luminaire #2 for horizontal plane at angle 45°.

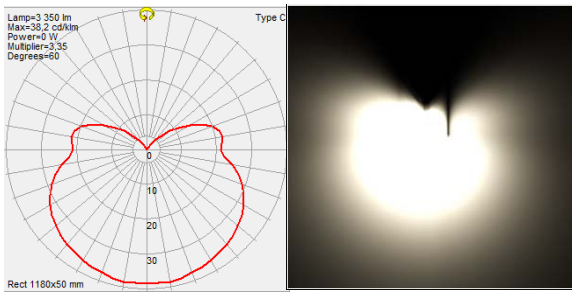

Figure 9.16: Luminaire exitance diagram and the rendered image for this description for luminaire #2 for horizontal plane at angle 60°.

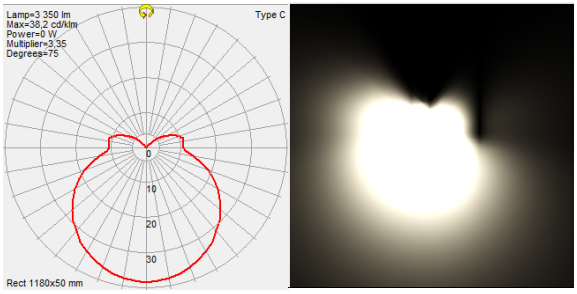

Figure 9.17: Luminaire exitance diagram and the rendered image for this description for luminaire #2 for horizontal plane at angle 75°.

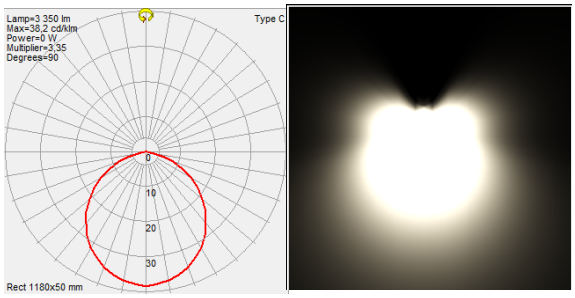

Figure 9.18: Luminaire exitance diagram and the rendered image for this description for luminaire #2 for horizontal plane at angle 90°.

Luminaire # 3

Basic parameters

Type:	Unknown producer	
Properties:	Length:	1242 mm
	Width:	175-200 mm
	Height:	100 mm
	Luminous intensity:	3.92 $[lumen \cdot m^{-2}]$
	Chromaticity temperature:	4000 [K]

Fluorescent Tube

Type: Radium NL 36W/21

Figure 9.19: Holder and cover for luminaire # 3.

Figure 9.20: Fluorescent tube for luminaire # 3.

Figure 9.21: Luminaire # 3 switched off.

Figure 9.22: Luminaire # 3 switched on.

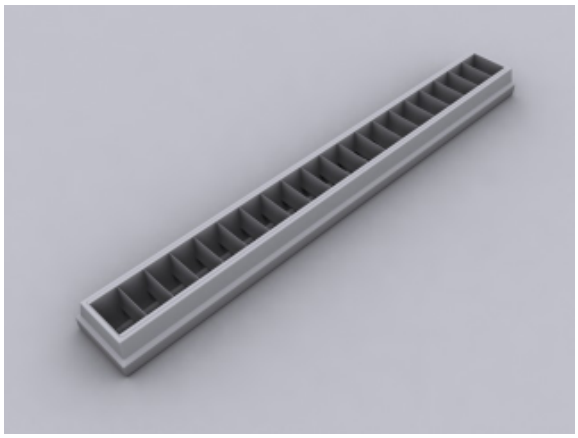

Figure 9.23: 3D Model svtidla # 3.

IESNA LM63-1995 description

```
IESNA file:
IESNA:LM-63-1995
[TEST] CTU Prague, Fel Katedra elektroenergetiky
[MANUFAC] unknown
[LUMCAT] unknown
[LUMINAIRE] Wall light with fluorescent light bulb lamp
[LAMP] Radium NL 36W/21
[DATE] 3.6.2008, Ing.Marek Balsky, Bc.Jiri Drahokoupil
[OTHER]
TILT=NONE
1 4100 1 19 3 1 2 10 1.242 17.5
1.0 1.0 36
0 5 10 15 20 25 30 35 40 45 50 55 60 65 70 75 80 85 90
0 45 90
1172 1179.72 1196.52 1136.4 1074.4 998.28 880.56 684.12 306.4 160.2
40.16 11.6 2.2 0 0 0 0 0 0
1172 1167 1183 1161 1098 1023 923 791 646 442 235 105.2 36.4 10.2 2.52
0 0 0 0
1172 1165 1154 1132 1102 1048 965 846 661 450.52 244.12 78.12 7.9 0 0
0 0 0 0
```

Luminaire diagrams

The spatial distribution of radiant intensity was measured in three horizontal planes positioned at 0°, 45° a 90°.

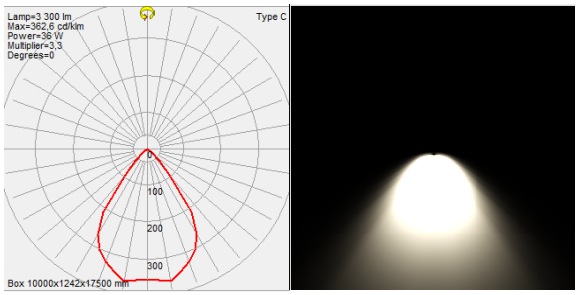

Figure 9.24: Luminaire radiant exitance diagram and the rendered image for this description for luminaire #2 for horizontal plane at angle 0°.

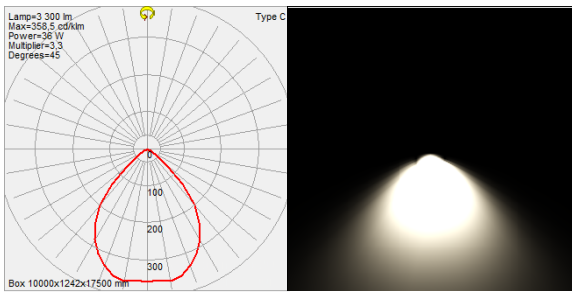

Figure 9.25: Luminaire radiant exitance diagram and the rendered image for this description for luminaire #2 for horizontal plane at angle 45°.

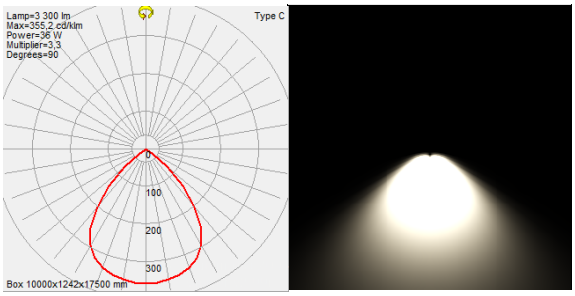

Figure 9.26: Luminaire radiant exitance diagram and the rendered image for this description for luminaire #2 for horizontal plane at angle 90°.

Luminaire # 4

Basic parameters

Type:	RJH-TS Halogen Spot HL500	
Properties:	Length:	185 mm
	Width:	145 mm
	Height:	122 mm
	Luminous intensity:	334.184 $[lumen \cdot m^{-2}]$
	Chromaticity temperature:	4000 [K]

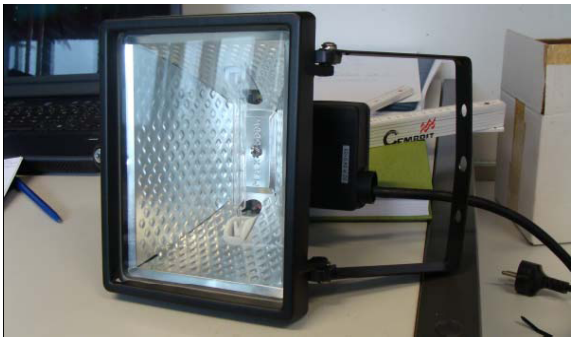

Figure 9.27: Body of luminaire # 4.

Figure 9.28: Luminaire # 4 switched off.

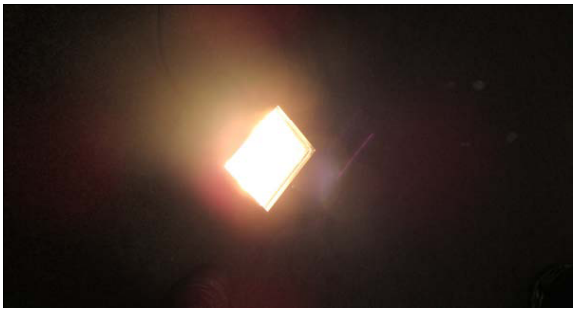

Figure 9.29: Luminaire # 4 switched on.

Figure 9.30: 3D Model of luminaire # 4.

IESNA LM63-1995 description

```
IESNA:LM-63-1995
[TEST] CTU Prague, FEL Katedra elektroenergetiky
[MANUFAC] Radium
[LUMCAT] Halogen Spot HL500
[LUMINAIRE] Halogen wall lamp
[LAMP] Radium RJH-TS 500W/230
[DATE] 3.6.2008, Ing.Marek Balsky, Bc.Jiri Drahokoupil
[OTHER]
TILT=NONE
1 9500 1 19 4 1 2 12.2 18.5 14.5
1.0 1.0 500.0
0 5 10 15 20 25 30 35 40 45 50 55 60 65 70 75 80 85 90
0 30 60 90
3532 3539 3590 3600 3611 3408 2946 2559 2126 1300 753.2 481.2 353.6
 252.6 172.8 103.4 43.2 18 4
3532 3548 3590 3551 3602 3587 3199 2693 2160 1816 1017 582.8 377
 264.92 175.6 105.32 70.8 14.92 2.3
3532 3522 3535 3508 3434 3331 3180 2823 2349 1737 1139 718.8 450.72
 270.2 187.4 111.12 51.5 16.32 3.4
3532 3539 3590 3600 3611 3408 2946 2559 2126 1300 753.2 481.2 353.6
 252.6 172.8 103.4 43.2 18 4
```

Luminaire diagrams

The spatial distribution of radiant intensity was measured in four horizontal planes positioned at 0°, 30°, 60°, and 90°.

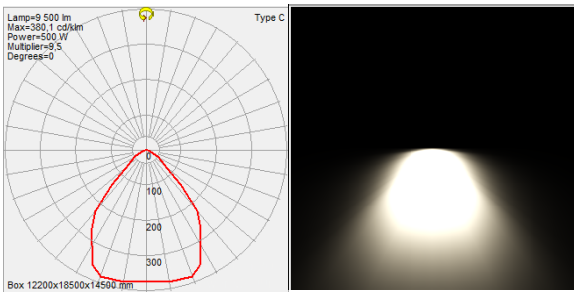

Figure 9.31: Luminaire radiant exitance diagram and the rendered image for this description for luminaire #2 for horizontal plane at angle 0°.

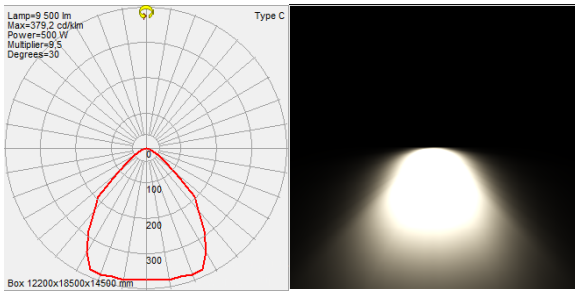

Figure 9.32: Luminaire radiant exitance diagram and the rendered image for this description for luminaire #2 for horizontal plane at angle 30°.

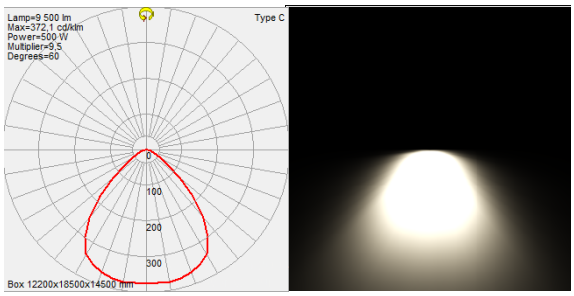

Figure 9.33: Luminaire radiant exitance diagram and the rendered image for this description for luminaire #2 for horizontal plane at angle 60°.

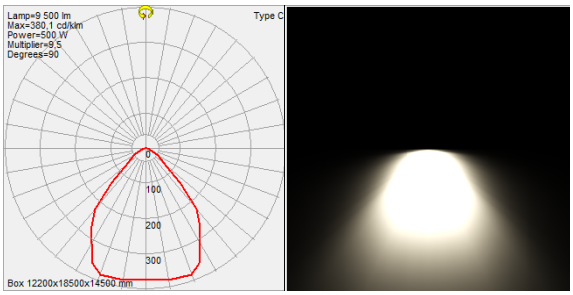

Figure 9.34: Luminaire radiant exitance diagram and the rendered image for this description for luminaire #2 for horizontal plane at angle 90°.

Luminaire # 5

Basic parameters

Type:	Philips	
Properties:	Maximum outer radius of luminaire corpus:	175 mm
	Minimum inner radius of luminaire corpus:	160 mm
	Length of the luminaire corpus	23.5 mm
	Length of luminaire body:	153 mm
	Height of luminaire body:	75 mm
	Width of luminaire body:	150 mm
	Luminous intensity:	37.95 $[lumen \cdot m^{-2}]$
	Chromaticity temperature:	2500 [K]

Gaseous Discharge Lamp

Type: Philips Master SDW-T 100W/825 PG12-1

Figure 9.35: Gaseous discharge lamp of luminaire # 5.

IESNA LM63-1995 description

```
IESNA:LM-63-1995
[TEST] CTU Prague, Fel Katedra elektroenergetiky
[MANUFAC] Philips
[LUMCAT] Philips
[LUMINAIRE] Discharge lamp with warm color to be used in open
luminairs
[LAMP] Philips Master SDW-T 100W/825 PG12-1
[DATE] 3.6.2008, Ing.Marek Balsky, Bc.Jiri Drahokoupil
[OTHER]
TILT=NONE
1 5000 1 19 1 1 2 -0.175 0 0
1.0 1.0 100
0 5 10 15 20 25 30 35 40 45 50 55 60 65 70 75 80 85 90
0
426 426.52 457 521.52 630 761 865 906 845 758 676 590.52 524.52 395.52
 192.4 65.2 46.6 28.32 7.8
```

Luminaire diagrams

As the radiant exitance is axial symmetric, the measurement has been carried out only for a single horizontal plane 0°.

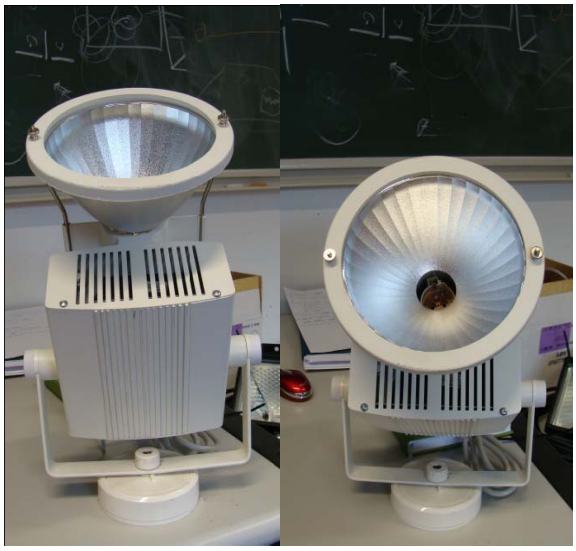

Figure 9.36: Body of luminaire # 5.

Figure 9.37: Luminaire #5 switched on and off.

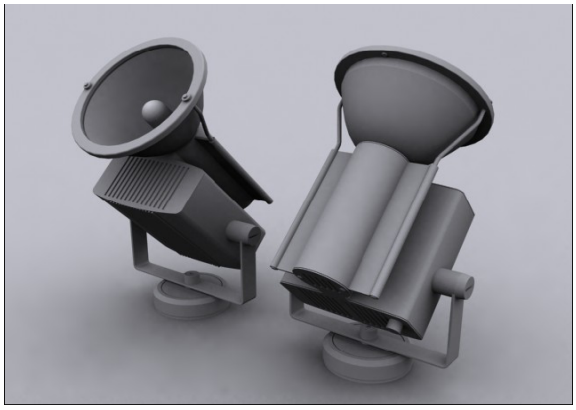

Figure 9.38: The 3D model of luminaire #3 with light shield.

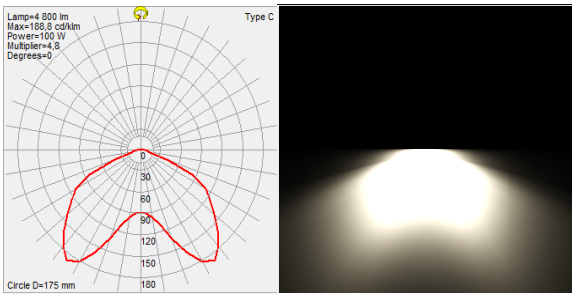

Figure 9.39: Luminaire radiant exitance diagram and the rendered image for this description for luminaire #2 for horizontal plane at angle 0°.

Luminaire # 6

Lamp type

Type:	Osram CONCENTRA PAR 38, E27, 80W	
Properties:	Mounting Length:	123 mm
	Length:	136 mm
	Diameter:	122 mm
	Beam angle	30 (degrees)
	Luminous intensity (cd): 1800	$[lumen \cdot m^{-2}]$
	Chromaticity temperature:	4000 [K]

The spare sample of this luminaire was not available. Therefore we use the goniometric diagram given by the lamp itself, there is an error due to the ommited simulation of light shield, but as this lamp was not switched on during the acquisition of HDR images, the error is irrelevant. Furthermore, the beam of the light is narrow, and hence it the error will be rather small even if the light is switch on.

Figure 9.40: Two photos of luminaire # 6 switched on.

Figure 9.41: 3D Model of luminaire # 6.

IESNA LM63-1995 description

```
IESNA:LM-63-1995
[TEST] CTU Prague, FEL Katedra elektroenergetiky
[MANUFAC] Osram
[LUMCAT] Osram
[LUMINAIRE] Reflector lamp
[LAMP] Osram CONCENTRA PAR 38, E27, 240V, 80W
[DATE] 3.6.2008, Ing.Marek Balsky, Bc.Jiri Drahokoupil
[OTHER]
TILT=NONE
1 1300 1 19 1 1 2 -0.18 0 0.16
1.0 1.0 80
0 5 10 15 20 25 30 35 40 45 50 55 60 65 70 75 80 85 90
0
1821.5 1559.4 1063.1 597.1 310.1 181.2 123.3 103.7 84.7 71.6 47.6 18.5 5.7 2.3
 1.1 1.2 0.9 0.7 0
```

Luminaire diagram

As the radiant exitance is axial symmetric, the measurement has been carried out only for a single horizontal plane 0°.

Note: the photometric diagram is available on the web of the OSRAM company and therefore this luminaire was a test to verify the accuracy of measurement. According to the technical sheet, the maximum luminous intensity is 1800 $lumen \cdot m^{-2}$, which corresponds well to the measured value 1821.5 $lumen \cdot m^{-2}$. This validates the accuracy of measurement for other five luminaires.

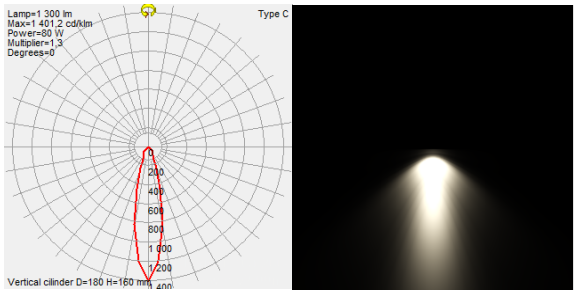

Figure 9.42: Luminaire radiant exitance diagram and the rendered image for this description for luminaire #6 for horizontal plane at angle 0°.

10 Appendix C - Surface Reflectances

In this appendix we describe the occurrence and assignment of surface reflectances (BRDFs) to the materials of objects in the MPI Informatics building model.

The surfaces of the MPI Informatics building model were assigned the reflectances. Due to the lack of resources the bidirectional reflectance distribution function (BRDF) for these materials used in the real building were not measured. Therefore, the reflectance was only estimated with the help of the reflectance database project CUReT [6] (Columbia-Utrecht Reflectance and Texture Database) that describes 61 materials in Oren-Nayar reflectance model. Based on this, fitting to physically Phong model was carried out and the results were visually compared with a photograph of a corresponding real object from the building. Even if this reflectance assignment is only rough approximation, the visual tests has shown relatively close fitting to the appearance of the real-world objects. This fitting can be further improved on.

Obviously, there is an option to measure the surface reflectances exactly in the future, but there is a problem of acquiring the samples of materials in the building for measurement, as the extraction of the sufficiently large planar material sample is infeasible (and not allowed by building administration). Therefore the appropriate method that can measure the BRDF in place without the necessity of extracting the sample should be used and perhaps even developed.

C-1 Material Sample BF_louisPoulsen

Usage:

Material used for transparent lamp-shade of Louis Poulsen luminaires (# 1).

Material properties

Material Type(PBRT)	translucent
Setting	Kd [0.9627 0.9627 0.9627] Ks [1.0 1.0 1.0] reflect [0.9627 0.9627 0.9627] transmit [0.9627 0.9627 0.9627] roughness [0.1]
Diffuse component in input VRML file	[0.8627 0.8627 0.8627]

The textual description in the material file

```
BF_louisPoulsen 0.8627 0.8627 0.8627 MAT-translucent Kd [ 0.9627 0.9627 0.9627 ]
                                                     Ks [ 1.0 1.0 1.0 ]
                                                     fl [ 0.9627 0.9627 0.9627 ]
                                                     r [ 0.1 ]
                                                     tt [ 0.9627 0.9627 0.9627 ]
```

Material appearance example

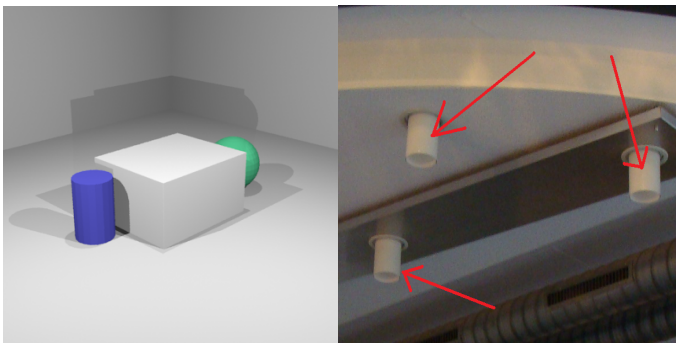

Figure 10.1: Example rendered with the material (left) and photo (right) for the material BF_louisPoulsen.

C-2 Material Sample BF_Alum01

Usage:

Shiny aluminum surfaces at the edge of white boards, the metallic dustbins.

Material properties

Material Type(PBRT)	shinymetal
Setting	roughness [0.9] Ks [0.5529 0.5529 0.5529] Kr [0.5529 0.5529 0.5529]
Diffuse component in input VRML file	[0.9529 0.9529 0.9529]

The textual description in the material file

```
BF_Alum01 0.9529 0.9529 0.9529 MAT-shiny r [0.9]
                                        Kr [0.9608 0.9608 0.9608]
                                        Ks [0.9608 0.9608 0.9608]
```

Material appearance example

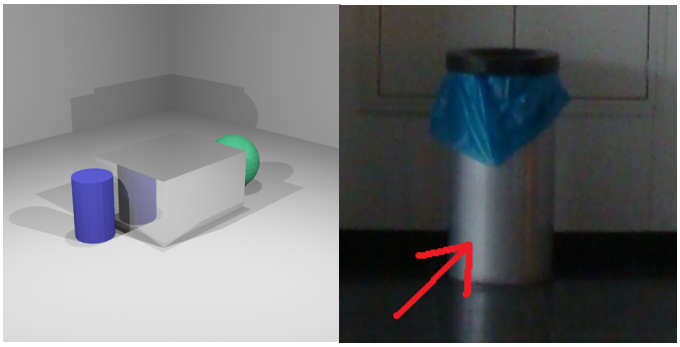

Figure 10.2: Image rendered with the material (left) and photo (right) for the material BF_Alum01.

C-3 Material Sample BF_black01

Usage:

Material used for plastic parts (washers, heel-pieces), matte plastic.

Material properties

Material Type(PBRT)	plastic
Setting	roughness [0.1] Kd [0.05 0.05 0.05] Ks [0.05 0.05 0.05]
Diffuse component in input VRML file	[0.07843 0.07843 0.07843]

The textual description in the material file

```
BF_black01 0.07843 0.07843 0.07843 MAT-plastic r [ 0.1 ]
                                               Kd [ 0.05 0.05 0.05 ]
                                               Ks [ 0.05 0.05 0.05 ]
```

Material appearance example

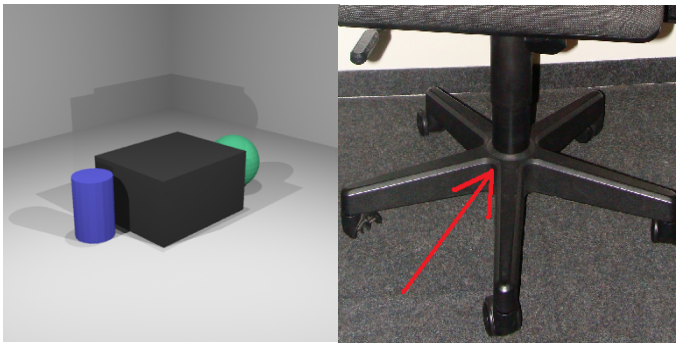

Figure 10.3: Image rendered with the material (left) and photo (right) for the material BF_black01.

C-4 Material Sample BF_black02

Usage:

Material used for the chair body (backrest and seat) for shiny black chairs.

Material properties

Material Type(PBRT)	matte
Setting	sigma [20.1223] Kd [0.05 0.05 0.05]
Diffuse component in input VRML file	[0.01176 0.01176 0.01176]

The textual description in the material file

```
BF_black02 0.01176 0.01176 0.01176 MAT-matte s [ 20.1223 ]
                                            Kd [ 0.05 0.05 0.05 ]
```

Material appearance example

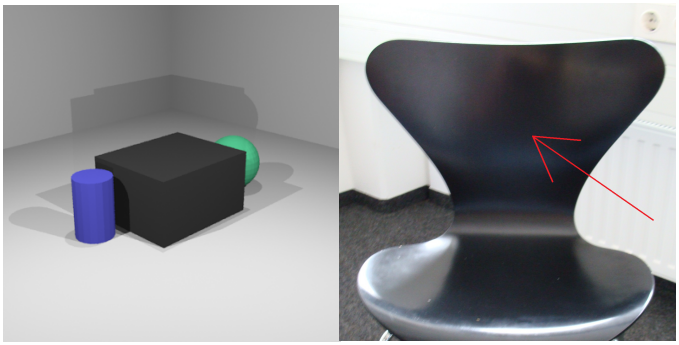

Figure 10.4: Image rendered with the material (left) and photo (right) for the material BF_black02.

C-5 Material Sample BF_black03

Usage:

Material for black leathered seats and chairs.

Material properties

Material Type(PBRT)	matte
Setting	sigma [10.3] Kd [0.01 0.01 0.01]
Diffuse component in input VRML file	[0.07059 0.07059 0.07059]

The textual description in the material file

```
BF_black03 0.07059 0.07059 0.07059 MAT-matte s [ 10.3 ]
                                           Kd [ 0.01 0.01 0.01 ]
```

Material appearance example

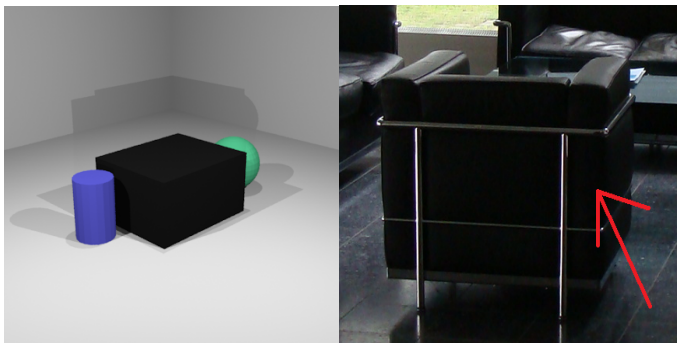

Figure 10.5: Image rendered with the material (left) and photo (right) for the material BF_black03.

C-6 Material Sample BF_black04

Usage:

Material used for metallic parts of furniture.

Material properties

Material Type(PBRT)	matte
Setting	sigma [29.39] Kd [0.302 0.302 0.302]
Diffuse component in input VRML file	[0.302 0.302 0.302]

The textual description in the material file

```
BF_black04 0.302 0.302 0.302 MAT-matte s [ 29.39 ]
                                       Kd [ 0.302 0.302 0.302 ]
```

Material appearance example

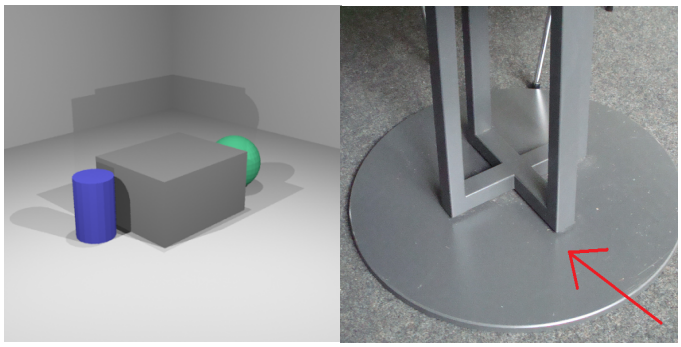

Figure 10.6: Image rendered with the material (left) and photo (right) for the material BF_black04.

C-7 Material Sample BF_black05

Usage:

Material use for black gum surface, for example for grab handle of fire extinguishers.

Material properties

Material Type(PBRT)	matte
Setting	sigma [17.189] Kd [0 0 0]
Diffuse component in input VRML file	[0 0 0]

The textual description in the material file

```
BF_black05 0 0 0 MAT-matte s [ 17.189 ] Kd [ 0 0 0 ]
```

Material appearance example

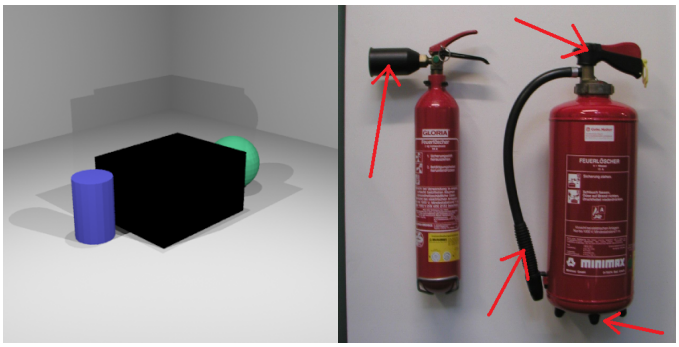

Figure 10.7: Image rendered with the material (left) and photo (right) for the material BF_black05.

C-8 Material Sample BF_blue01

Usage:

Material use for plastic heel-pieces and jointing, for example white boards.

Material properties

Material Type(PBRT)	plastic
Setting	roughness [0.6] Kd [0.0902 0.07843 0.5804] Ks [0.0902 0.07843 0.5804]
Diffuse component in input VRML file	[0.0902 0.07843 0.5804]

The textual description in the material file

```
BF_blue01 0.0902 0.07843 0.5804 MAT-plastic r [ 0.6 ]
                                            Kd [ 0.0902 0.07843 0.5804 ]
                                            Ks [ 0.0902 0.07843 0.5804 ]
```

Material appearance example

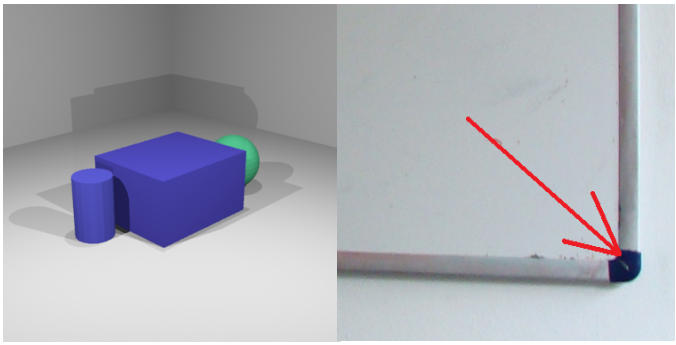

Figure 10.8: Image rendered with the material (left) and photo (right) for the material BF_blue01.

C-9 Material Sample BF_blue02

Usage:

Material used for plastic chairs in the coffee bar in the first floor.

Material properties

Material Type(PBRT)	plastic
Setting	roughness [0.1] Kd [0.08 0.08 0.4] Ks [0.08 0.08 0.4]
Diffuse component in input VRML file	[0.2353 0.2431 0.6863]

The textual description in the material file

```
BF_blue02 0.2353 0.2431 0.6863 MAT-plastic r [ 0.1 ]
                                           Kd [ 0.08 0.08 0.4 ]
                                           Ks [ 0.08 0.08 0.4 ]
```

Material appearance example

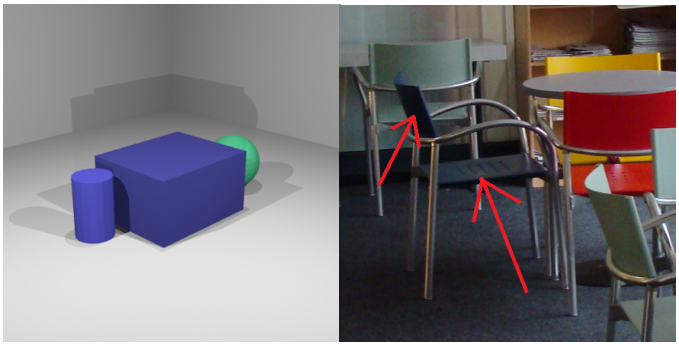

Figure 10.9: Image rendered with the material (left) and photo (right) for the material BF_blue02.

C-10 Material Sample BF_bolts01

Usage:

Material used for metallic screws and bolts.

Material properties

Material Type(PBRT)	shinymetal
Setting	roughness [0.9] Kr [0.9 0.9 0.9] Ks [1.0 1.0 1.0]
Diffuse component in input VRML file	[0.8824 0.8824 0.8824]

The textual description in the material file

```
BF_bolts01 0.8824 0.8824 0.8824 MAT-shiny r [ 0.9 ]
                                        Kr [ 0.9 0.9 0.9 ]
                                        Ks [ 1.0 1.0 1.0 ]
```

Material appearance example

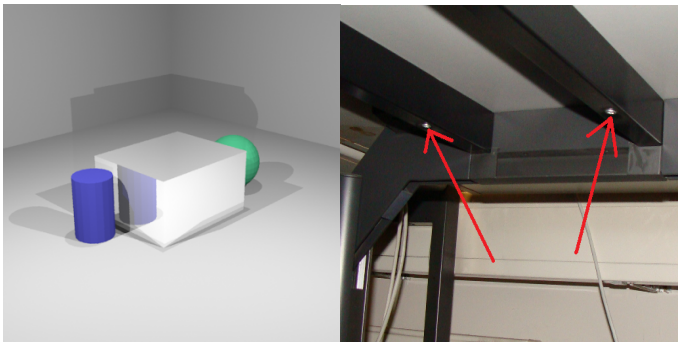

Figure 10.10: Image rendered with the material (left) and photo (right) for the material BF_bolts01.

C-11 Material Sample BF_brMetal01

Usage:

Material used for grab handles, cribs, and chair frames.

Material properties

Material Type(PBRT)	shinymetal
Setting	roughness [1.0] Ks [0.5 0.5 0.5] Kr [0.5 0.5 0.5]
Diffuse component in input VRML file	[0.9137 0.9137 0.9137]

The textual description in the material file

```
BF_brMetal01 0.9137 0.9137 0.9137 MAT-shiny r [ 1.0 ]
                                          Ks [ 0.5 0.5 0.5 ]
                                          Kr [ 0.5 0.5 0.5 ]
```

Material appearance example

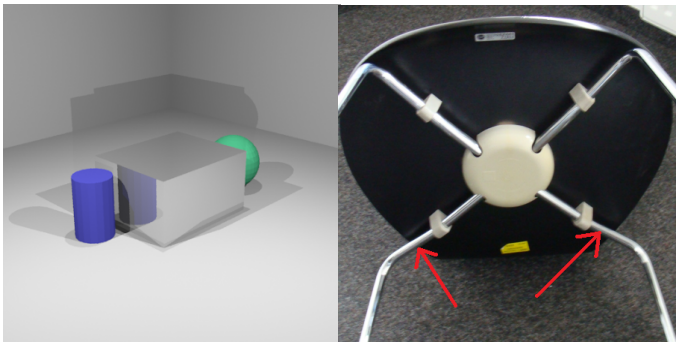

Figure 10.11: Image rendered with the material (left) and photo (right) for the material BF_brMetal01.

C-12 Material Sample BF_brown01

Usage:

Material used as filling of cork boards.

Material properties

Material Type(PBRT)	matte
Setting	sigma [10.30] Kd [0.5373 0.2235 0.04235]
Diffuse component in input VRML file	[0.7373 0.4235 0.08235]

The textual description in the material file

```
BF_brown01 0.7373 0.4235 0.08235 MAT-matte s [ 10.30 ]
                                          Kd [ 0.5373 0.2235 0.04235 ]
```

Material appearance example

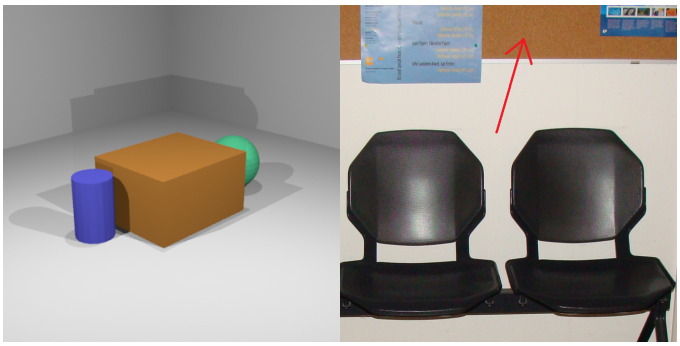

Figure 10.12: Image rendered with the material (left) and photo (right) for the material BF_brown01.

C-13 Material Sample BF_cream01

Usage:

Material used for the frames of green boards.

Material properties

Material Type(PBRT)	plastic
Setting	roughness [0.1] Kd [0.8745 0.8667 0.7882] Ks [1.0 1.0 1.0]
Diffuse component in input VRML file	[0.8745 0.8667 0.7882]

The textual description in the material file

```
BF_cream01 0.8745 0.8667 0.7882 MAT-plastic r [ 0.1 ]
                                            Kd [ 0.8745 0.8667 0.7882 ]
                                            Ks [ 1.0 1.0 1.0 ]
```

Material appearance example

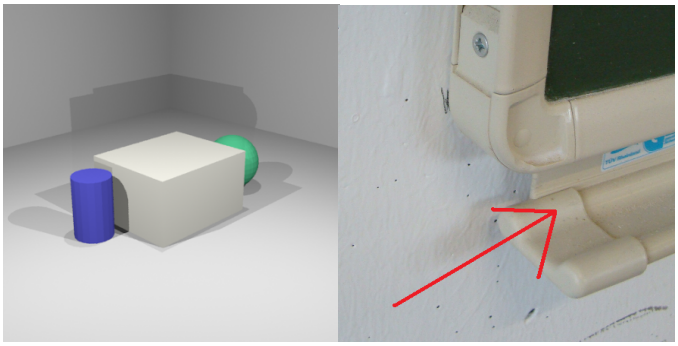

Figure 10.13: Image rendered with the material (left) and photo (right) for the material BF_cream01.

C-14 Material Sample BF_foxiness01

Usage:

Material used for throttle-valves of fire extinguishers and heating parts (cock-metal).

Material properties

Material Type(PBRT)	substrate
Setting	Kd [0.751 0.2922 0.06667] Ks [0.751 0.2922 0.06667] uroughness [0.3] vroughness [0.2]
Diffuse component in input VRML file	[0.651 0.3922 0.06667]

The textual description in the material file

```
BF_foxiness01 0.651 0.3922 0.06667 MAT-substrate Kd [ 0.751 0.2922 0.06667 ]
                                                 Ks [ 0.751 0.2922 0.06667 ]
                                                 ur [ 0.3 ] vr [ 0.2 ]
```

Material appearance example

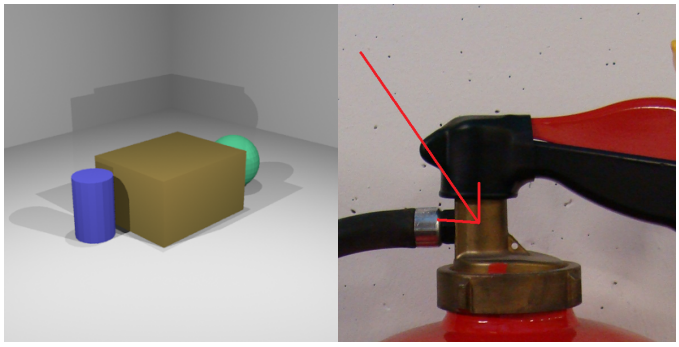

Figure 10.14: Image rendered with the material (left) and photo (right) for the material BF_foxiness01.

C-15 Material Sample BF_glass01

Usage:

Material used as glass filling of a round table.

Material properties

Material Type(PBRT)	glass
Setting	index [1.5] Kr [1.0 1.0 1.0] Kt [0.8 0.8 0.8]
Diffuse component in input VRML file	[0.7255 0.7255 0.7255]

The textual description in the material file

```
BF_glass01 0.7255 0.7255 0.7255 MAT-glass in [ 1.5 ]
                                         Kr [ 1.0 1.0 1.0 ]
                                         Kt [ 0.8 0.8 0.8 ]
```

Material appearance example

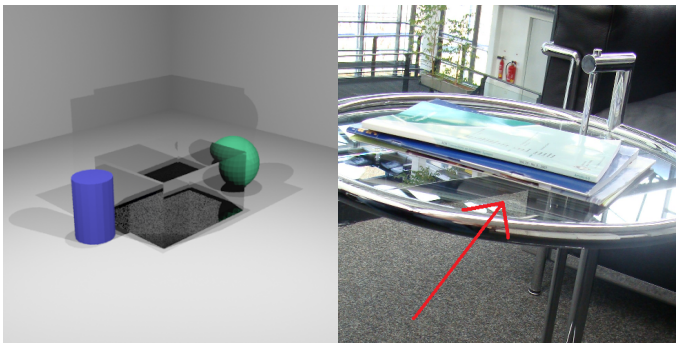

Figure 10.15: Image rendered with the material (left) and photo (right) for the material BF_glass01.

C-16 Material Sample BF_gray01

Usage:

Material used for metallic parts of stair-rails and other constructions.

Material properties

Material Type(PBRT)	matte
Setting	sigma [40.1072] Kd [0.2 0.2 0.4]
Diffuse component in input VRML file	[0.3765 0.3765 0.549]

The textual description in the material file

```
BF_gray01 0.3765 0.3765 0.549 MAT-matte s [ 40.1072 ]
                                        Kd [ 0.2 0.2 0.4 ]
```

Material appearance example

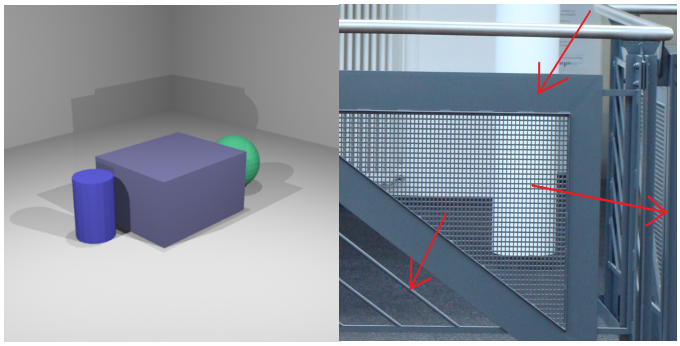

Figure 10.16: Image rendered with the material (left) and photo (right) for the material BF_gray01.

C-17 Material Sample BF_gray02

Usage:

Material used for support of office furniture.

Material properties

Material Type(PBRT)	plastic
Setting	roughness [0.6] Kd [0.1 0.1 0.15] Ks [0.1 0.1 0.15]
Diffuse component in input VRML file	[0.2941 0.2941 0.2941]

The textual description in the material file

```
BF_gray02 0.2941 0.2941 0.2941 MAT-plastic  r [ 0.6 ]
                                            Kd [ 0.1 0.1 0.15 ]
                                            Ks [ 0.1 0.1 0.15 ]
```

Material appearance example

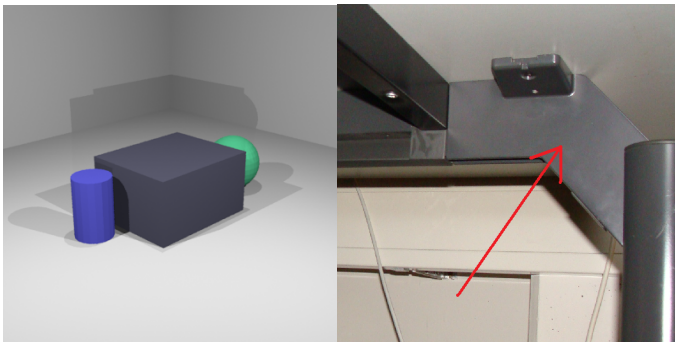

Figure 10.17: Image rendered with the material (left) and photo (right) for the material BF_gray02.

C-18 Material Sample BF_gray03

Usage:

Material used for plastic backrest of metallic sitting benches.

Material properties

Material Type(PBRT)	plastic
Setting	roughness [0.05] Kd [0.0804 0.0765 0.0922] Ks [0.0804 0.0765 0.0922]
Diffuse component in input VRML file	[0.1804 0.1765 0.1922]

The textual description in the material file

```
BF_gray03 0.1804 0.1765 0.1922 MAT-plastic  r [ 0.05 ]
                                            Kd [ 0.0804 0.0765 0.0922 ]
                                            Ks [ 0.0804 0.0765 0.0922 ]
```

Material appearance example

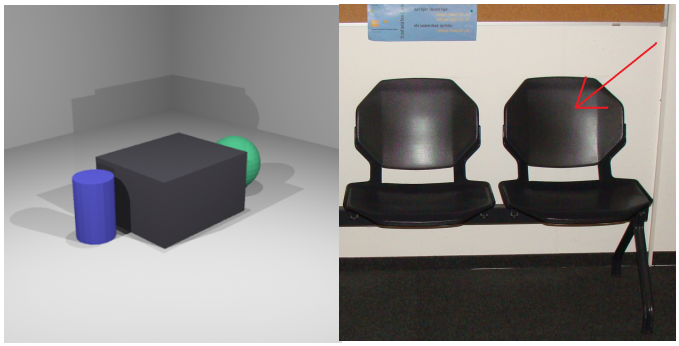

Figure 10.18: Image rendered with the material (left) and photo (right) for the material BF_gray03.

C-19 Material Sample BF_gray04

Usage:

Material used for majority of office furniture surfaces.

Material properties

Material Type(PBRT)	uber
Setting	Kd [0.4824 0.4824 0.4824] Ks [0.8824 0.8824 0.8824] Kr [0.0224 0.0224 0.0224] roughness [ ]
Diffuse component in input VRML file	[]

The textual description in the material file

```
BF_gray04 0.6824 0.6824 0.6824 MAT-uber Kd [ 0.4824 0.4824 0.4824 ]
                                        Ks [ 0.8824 0.8824 0.8824 ]
                                        Kr [ 0.0224 0.0224 0.0224 ]
                                        r [ 1.0 ]
```

Material appearance example

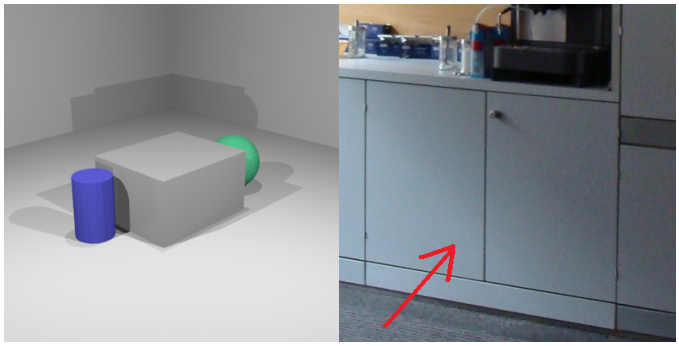

Figure 10.19: Image rendered with the material (left) and photo (right) for the material BF_gray04.

C-20 Material Sample BF_green01

Usage:

Material used for the interior of green boards.

Material properties

Material Type(PBRT)	matte
Setting	sigma [17.699] Kd [0.02 0.02 0.02]
Diffuse component in input VRML file	[0.03922 0.3137 0.03922]

The textual description in the material file

```
BF_green01 0.03922 0.3137 0.03922 MAT-matte s [ 17.699 ]
                                            Kd [ 0.02 0.2 0.02 ]
```

Material appearance example

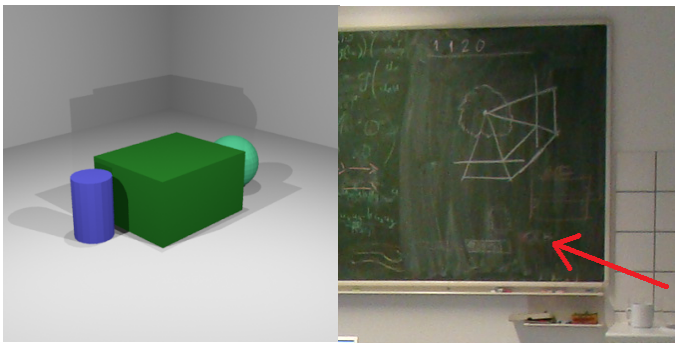

Figure 10.20: Image rendered with the material (left) and photo (right) for the material BF_green01.

C-21 Material Sample BF_green02

Usage:

Material used for the seat filling of green chairs in the rondell.

Material properties

Material Type(PBRT)	matte
Setting	sigma [23.76] Kd [0.4 0.95 0.6]
Diffuse component in input VRML file	[0.5843 0.8784 0.7765]

The textual description in the material file

```
BF_green02 0.5843 0.8784 0.7765 MAT-matte s [ 23.76 ]
                                          Kd [ 0.4 0.95 0.6 ]
```

Material appearance example

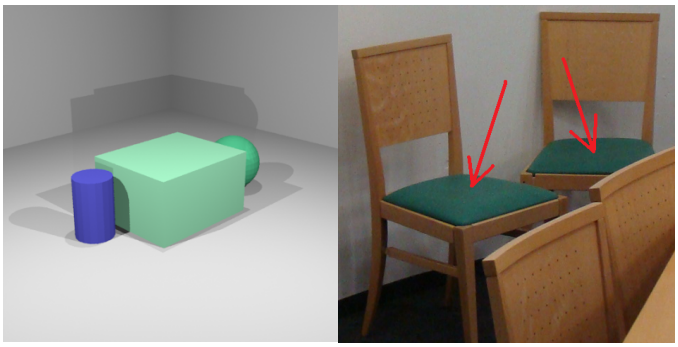

Figure 10.21: Image rendered with the material (left) and photo (right) for the material BF_green02.

C-22 Material Sample BF_green03

Usage:

Material used for plastic chairs in the coffee bar in the first floor.

Material properties

Material Type(PBRT)	plastic
Setting	roughness [0.1] Kd [0.7608 0.9765 0.8667] Ks [0.7608 0.9765 0.8667]
Diffuse component in input VRML file	[0.7608 0.9765 0.8667]

The textual description in the material file

```
BF_green03 0.7608 0.9765 0.8667 MAT-plastic r [ 0.1 ]
                                            Kd [ 0.7608 0.9765 0.8667 ]
                                            Ks [ 0.7608 0.9765 0.8667 ]
```

Material appearance example

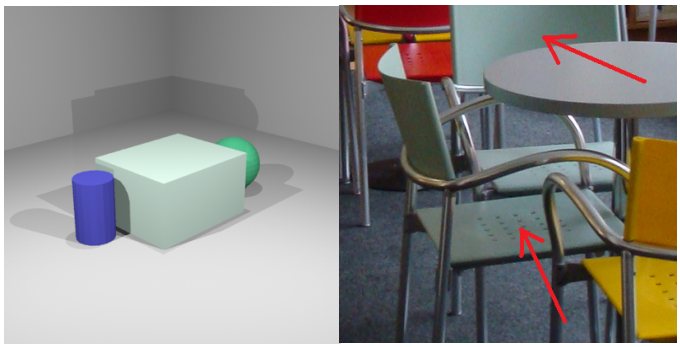

Figure 10.22: Image rendered with the material (left) and photo (right) for the material BF_green03.

C-23 Material Sample BF_red01

Usage:

Material used for the metallic body of fire extinguishers.

Material properties

Material Type(PBRT)	shinymetal
Setting	roughness [0.9] Ks [0.8 0.2 0.1] Kr [0.8 0.2 0.1]
Diffuse component in input VRML file	[0.8196 0.2 0.09804]

The textual description in the material file

```
BF_red01 0.8196 0.2 0.09804 MAT-shiny r [ 0.9 ]
                                    Ks [ 0.8 0.2 0.1 ]
                                    Kr [ 0.8 0.2 0.1 ]
```

Material appearance example

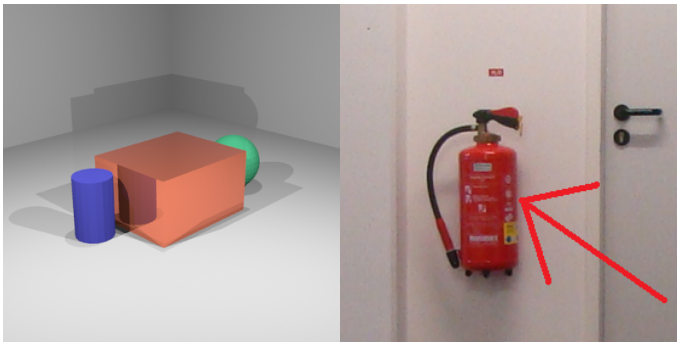

Figure 10.23: Image rendered with the material (left) and photo (right) for the material BF_red01.

C-24 Material Sample BF_red02

Usage:

Material used for the metallic body of fire extinguishers (CO_2).

Material properties

Material Type(PBRT)	shinymetal
Setting	roughness [1.0] Ks [0.9 0.05 0.05] Kr [0.9 0.05 0.05]
Diffuse component in input VRML file	[0.8627 0.1137 0.1922]

The textual description in the material file

```
BF_red02 0.8627 0.1137 0.1922 MAT-shiny r [ 1.0 ]
                                          Ks [ 0.9 0.05 0.05 ]
                                          Kr [ 0.9 0.05 0.05 ]
```

Material appearance example

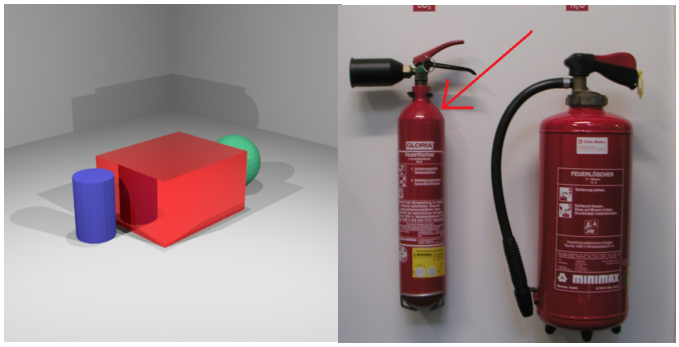

Figure 10.24: Image rendered with the material (left) and photo (right) for the material BF_red02.

C-25 Material Sample BF_red03

Usage:

Material used for plastic chairs in the coffee bar in the first floor.

Material properties

Material Type(PBRT)	plastic
Setting	roughness [0.1] Kd [0.902 0.05 0.05] Ks [0.902 0.05 0.05]
Diffuse component in input VRML file	[0.902 0.2 0.2]

The textual description in the material file

```
BF_red03 0.902 0.2 0.2 MAT-plastic r [ 0.1 ]
                                   Kd [ 0.902 0.05 0.05 ]
                                   Ks [ 0.902 0.05 0.05 ]
```

Material appearance example

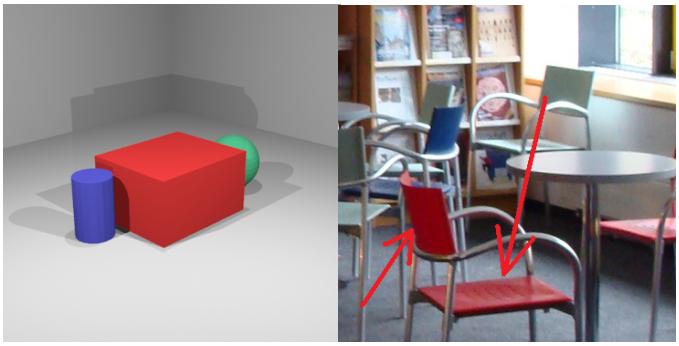

Figure 10.25: Image rendered with the material (left) and photo (right) for the material BF_red03.

C-26 Material Sample BF_redBrown01

Usage:

Material used for the bolstering of office wheel-chairs (backrest and seat).

Material properties

Material Type(PBRT)	matte
Setting	sigma [35.179] Kd [0.6549 0.4118 0.3765]
Diffuse component in input VRML file	[0.4549 0.4118 0.3765]

The textual description in the material file

```
BF_redBrown01 0.4549 0.4118 0.3765 MAT-matte s [ 35.179 ]
                                              Kd [ 0.6549 0.4118 0.3765 ]
```

Material appearance example

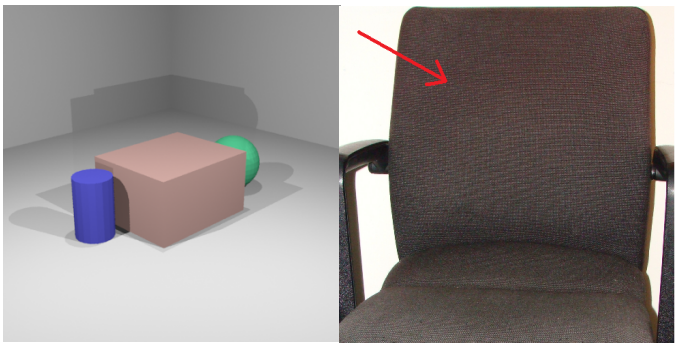

Figure 10.26: Image rendered with the material (left) and photo (right) for the material BF_redBrown01.

C-27 Material Sample BF_shMetal01

Usage:

Material used for metallic parts of chairs (chair-frame).

Material properties

Material Type(PBRT)	shiny
Setting	roughness [0.3] Ks [0.9 0.9 0.9] Kr [0.9 0.9 0.9]
Diffuse component in input VRML file	[0.949 0.949 0.949]

The textual description in the material file

```
BF_shMetal01 0.949 0.949 0.949 MAT-shiny r [ 0.3 ]
                                        Ks [ 0.9 0.9 0.9 ]
                                        Kr [ 0.9 0.9 0.9 ]
```

Material appearance example

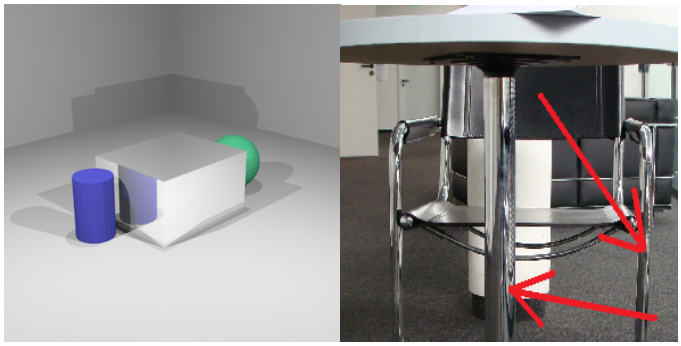

Figure 10.27: Image rendered with the material (left) and photo (right) for the material BF_shMetal01.

C-28 Material Sample BF_white01

Usage:

Material used as the filling of white boards.

Material properties

Material Type(PBRT)	plastic
Setting	roughness [0.2] Kd [0.9608 0.9608 0.9608] Ks [0.9608 0.9608 0.9608]
Diffuse component in input VRML file	[0.9608 0.9608 0.9608]

The textual description in the material file

```
BF_white01 0.9608 0.9608 0.9608 MAT-plastic r [ 0.2 ]
                                            Kd [ 0.9608 0.9608 0.9608 ]
                                            Ks [ 0.9608 0.9608 0.9608 ]
```

Material appearance example

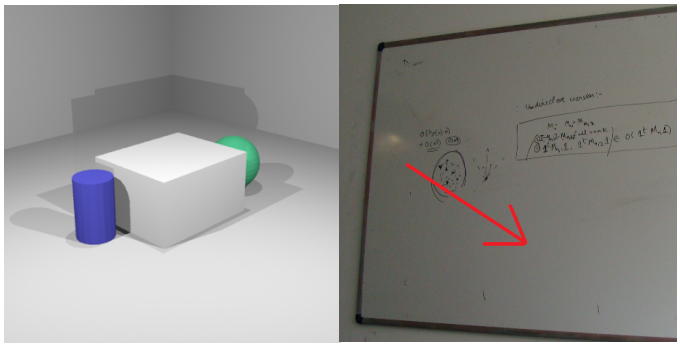

Figure 10.28: Image rendered with the material (left) and photo (right) for the material BF_white01.

C-29 Material Sample BF_white02

Usage:

Material used as the trestle-board of the solid round table.

Material properties

Material Type(PBRT)	plastic
Setting	roughness [0.9] Kd [0.92 0.92 0.92] Ks [0.92 0.92 0.92]
Diffuse component in input VRML file	[0.9176 0.9176 0.9176]

The textual description in the material file

```
BF_white02 0.9176 0.9176 0.9176 MAT-plastic r [ 0.9 ]
                                            Kd [ 0.92 0.92 0.92 ]
                                            Ks [ 0.92 0.92 0.92 ]
```

Material appearance example

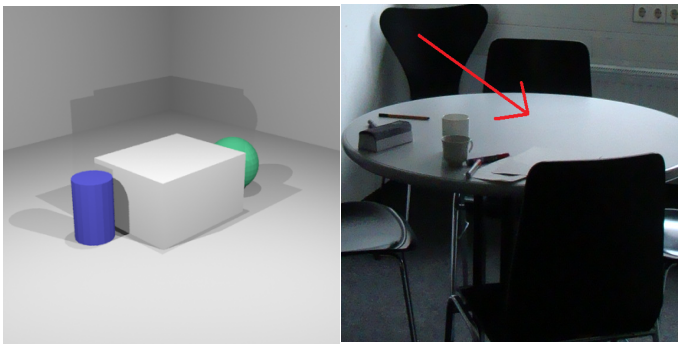

Figure 10.29: Image rendered with the material (left) and photo (right) for the material BF_white02.

C-30 Material Sample BF_wood01

Usage:

Material used for the wooden parts of sitting chairs in the rondell.

Material properties

Material Type(PBRT)	matte
Setting	sigma [20.128] Kd [0.9 0.6686 0.2078]
Diffuse component in input VRML file	[0.8627 0.7686 0.6078]

The textual description in the material file

```
BF_wood01 0.8627 0.7686 0.6078 MAT-matte s [ 20.128 ]
                                         Kd [ 0.9 0.6686 0.2078 ]
```

Material appearance example

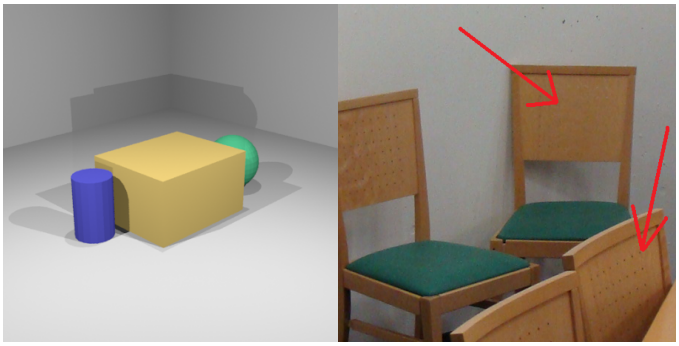

Figure 10.30: Image rendered with the material (left) and photo (right) for the material BF_wood01.

C-31 Material Sample BF_yellow01

Usage:

Material used for plastic chairs in the coffee bar in the first floor.

Material properties

Material Type(PBRT)	matte
Setting	sigma [15.928] Kd [0.8216 0.8333 0]
Diffuse component in input VRML file	[0.9216 0.9333 0]

The textual description in the material file

```
BF_yellow01 0.9216 0.9333 0 MAT-matte s [ 15.928 ]
                                      Kd [ 0.8216 0.8333 0 ]
```

Material appearance example

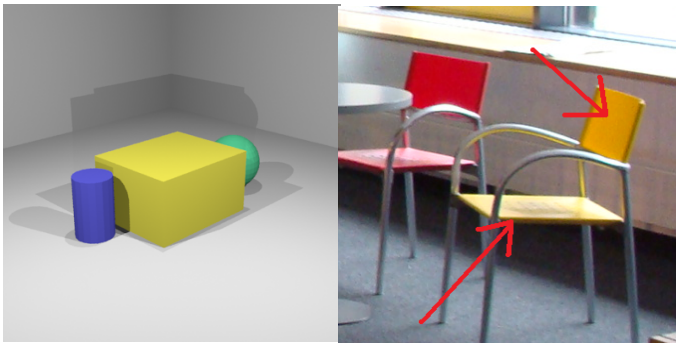

Figure 10.31: Image rendered with the material (left) and photo (right) for the material BF_yellow01.

C-32 Material Sample CH_alum01

Usage:

Material used for the frame holders of luminaires in the rondell.

Material properties

Material Type(PBRT)	shinymetal
Setting	roughness [1.0] Ks [0.5373 0.5373 0.5373] Kr [0.5373 0.5373 0.5373]
Diffuse component in input VRML file	[0.7373 0.7373 0.7373]

The textual description in the material file

```
CH_alum01 0.7373 0.7373 0.7373 MAT-shiny r [ 1.0 ]
                               Ks [ 0.5373 0.5373 0.5373 ]
                               Kr [ 0.5373 0.5373 0.5373 ]
```

Material appearance example

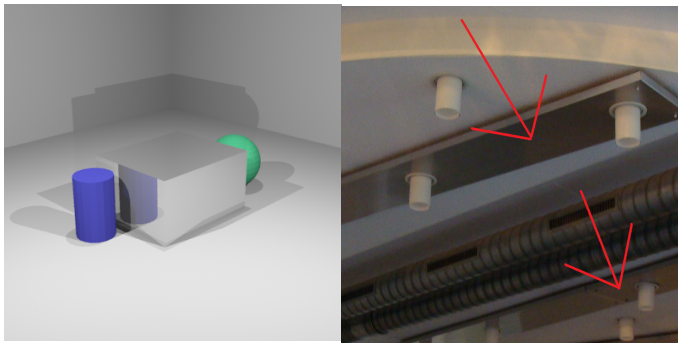

Figure 10.32: Image rendered with the material (left) and photo (right) for the material CH_alum01.

C-33 Material Sample CH_alum02

Usage:

Material used for metallic parts of ventilation.

Material properties

Material Type(PBRT)	uber
Setting	roughness [1.0] Kd [0.6451 0.6451 0.6451] Ks [0.2 0.2 0.2] Kr [0.05 0.05 0.05]
Diffuse component in input VRML file	[0.7452 0.7452 0.7452]

The textual description in the material file

```
CH_alum02 0.7452 0.7452 0.7452 MAT-uber r [ 1.0 ]
                                        Kd [ 0.6451 0.6451 0.6451 ]
                                        Ks [ 0.2 0.2 0.2 ]
                                        Kr [ 0.05 0.05 0.05 ]
```

Material appearance example

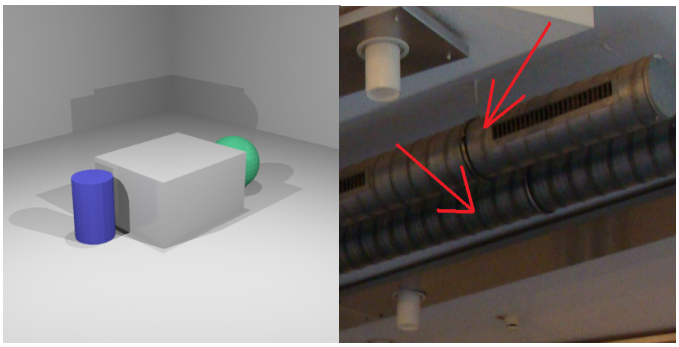

Figure 10.33: Image rendered with the material (left) and photo (right) for the material CH_alum02.

C-34 Material Sample CH_alum03

Usage:

Material used for metallic doors and parts of the lift.

Material properties

Material Type(PBRT)	shinymetal
Setting	roughness [1.0] Ks [0.4588 0.4588 0.4588] Kr [0.4588 0.4588 0.4588]
Diffuse component in input VRML file	[0.6588 0.6588 0.6588]

The textual description in the material file

```
CH_alum03 0.6588 0.6588 0.6588 MAT-shiny r [ 1.0 ]
                                        Ks [ 0.4588 0.4588 0.4588 ]
                                        Kr [ 0.4588 0.4588 0.4588 ]
```

Material appearance example

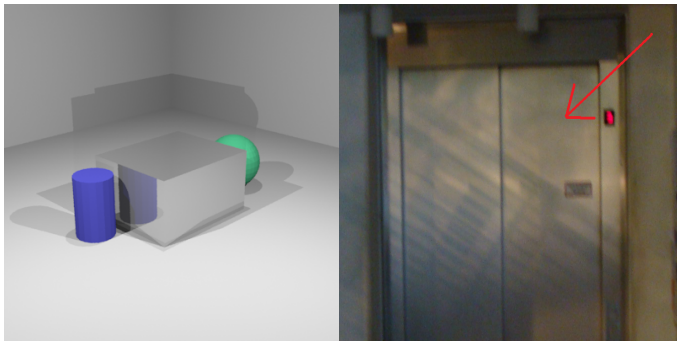

Figure 10.34: Image rendered with the material (left) and photo (right) for the material CH_alum03.

C-35 Material Sample CH_black01

Usage:

Material used for the seats of backrest of chesterfields and couches.

Material properties

Material Type(PBRT)	uber
Setting	roughness [1.0] Kd [0.0084 0.0084 0.0084] Ks [0.01 0.01 0.01] Kr [0.01 0.01 0.01]
Diffuse component in input VRML file	[0.1843 0.1843 0.1843]

The textual description in the material file

```
CH_black01 0.1843 0.1843 0.1843 MAT-uber Kd [ 0.0084 0.0084 0.0084 ]
                                         Ks [ 0.01 0.01 0.01 ]
                                         Kr [ 0.01 0.01 0.01 ]
                                         r [ 1.0 ]
```

Material appearance example

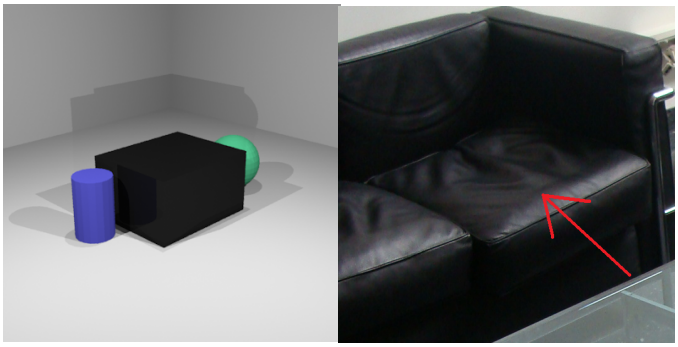

Figure 10.35: Image rendered with the material (left) and photo (right) for the material CH_black01.

C-36 Material Sample CH_black02

Usage:

Material used for the door pulling handle made of metal.

Material properties

Material Type(PBRT)	plastic
Setting	roughness [0.7] Kd [0.03 0.03 0.03] Ks [1.0 1.0 1.0]
Diffuse component in input VRML file	[0.1961 0.1961 0.1961]

The textual description in the material file

```
CH_black02 0.1961 0.1961 0.1961 MAT-plastic r [ 0.7 ]
                                            Kd [ 0.03 0.03 0.03 ]
                                            Ks [ 1.0 1.0 1.0 ]
```

Material appearance example

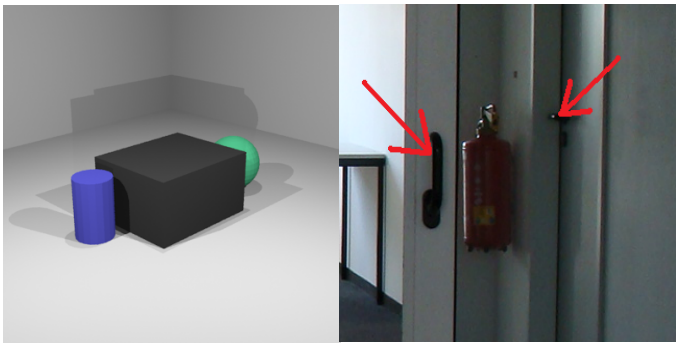

Figure 10.36: Image rendered with the material (left) and photo (right) for the material CH_black02.

C-37 Material Sample CH_constructionC01

Usage:

Material used for metallic frames around the plants and trees in the ground floor.

Material properties

Material Type(PBRT)	uber
Setting	Kd [0.02098 0.02843 0.04412] Ks [0.1 0.1 0.1] Kr [0.02098 0.02843 0.04412] roughness [1.0]
Diffuse component in input VRML file	[0.05098 0.07843 0.1412]

The textual description in the material file

```
CH_constructionC01 0.05098 0.07843 0.1412 MAT-uber r [ 1.0 ]
                                                  Kd [ 0.02098 0.02843 0.04412 ]
                                                  Ks [ 0.1 0.1 0.1 ]
                                                  Kr [ 0.02098 0.02843 0.04412 ]
```

Material appearance example

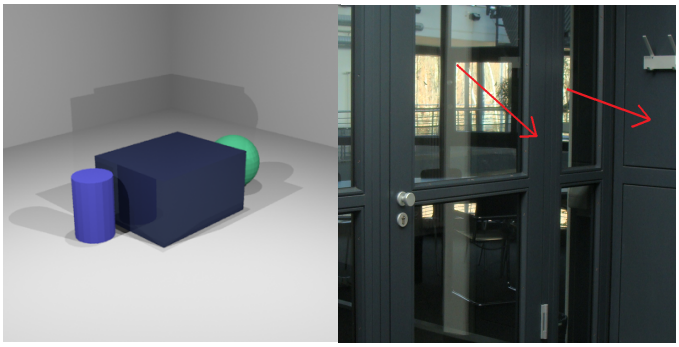

Figure 10.37: Image rendered with the material (left) and photo (right) for the material CH_constructionC01.

C-38 Material Sample CH_glass01

Usage:

Material used as glass for the doors and windows.

Material properties

Material Type(PBRT)	glass
Setting	Kr [1.0 1.0 1.0] Kt [0.8235 0.851 0.8824] index [1.5]
Diffuse component in input VRML file	[0.8235 0.851 0.8824]

The textual description in the material file

```
CH_glass01 0.8235 0.851 0.8824 MAT-glass Kr [ 1.0 1.0 1.0 ]
                                         Kt [ 0.8235 0.851 0.8824 ]
                                         in [ 1.5 ]
```

Material appearance example

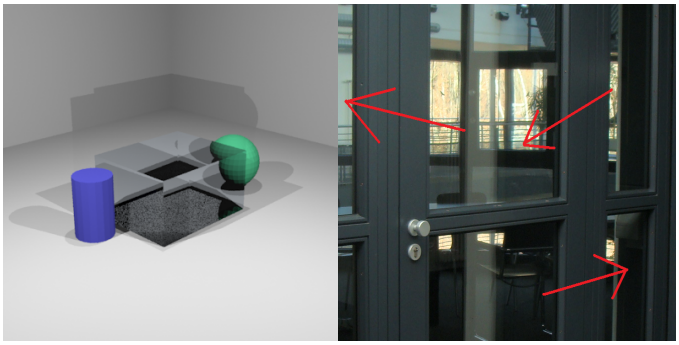

Figure 10.38: Image rendered with the material (left) and photo (right) for the material CH_glass01.

C-39 Material Sample CH_glass02

Usage:

Material used as glass for the filling in handrails.

Material properties

Material Type(PBRT)	glass
Setting	Kr [1.0 1.0 1.0] Kt [0.8882 0.8882 0.9359] index [1.1]
Diffuse component in input VRML file	[0.5882 0.5882 0.7059]

The textual description in the material file

```
CH_glass02 0.5882 0.5882 0.7059 MAT-glass Kr [ 1.0 1.0 1.0 ]
                                          Kt [ 0.8882 0.8882 0.9359 ]
                                          in [ 1.1 ]
```

Material appearance example

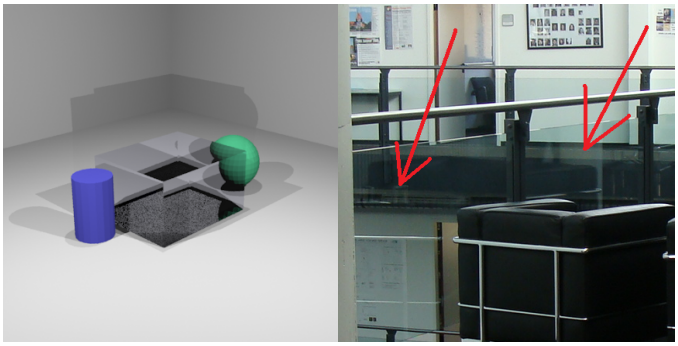

Figure 10.39: Image rendered with the material (left) and photo (right) for the material CH_glass02.

C-40 Material Sample CH_gray02

Usage:

Material used for the office doors.

Material properties

Material Type(PBRT)	plastic
Setting	roughness [0.9] Kd [0.8 0.8 0.8] Ks [0.8 0.8 0.8]
Diffuse component in input VRML file	[0.7451 0.7451 0.7451]

The textual description in the material file

```
CH_gray02 0.7451 0.7451 0.7451 MAT-plastic r [ 0.9 ]
                                           Kd [ 0.8 0.8 0.8 ]
                                           Ks [ 0.8 0.8 0.8 ]
```

Material appearance example

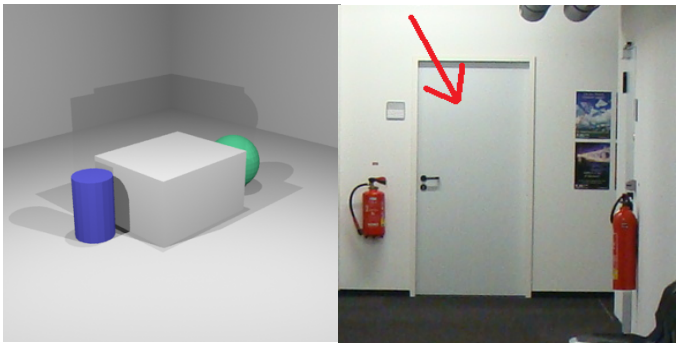

Figure 10.40: Image rendered with the material (left) and photo (right) for the material CH_gray02.

C-41 Material Sample CH_gray03

Usage:

Material used as the carpet in the offices and corridors.

Material properties

Material Type(PBRT)	matte
Setting	sigma [32.456] Kd [0.0725 0.0725 0.1353]
Diffuse component in input VRML file	[0.1725 0.1725 0.2353]

The textual description in the material file

```
CH_gray03 0.1725 0.1725 0.2353 MAT-matte s [ 32.456 ]
                                        Kd [ 0.0725 0.0725 0.1353 ]
```

Material appearance example

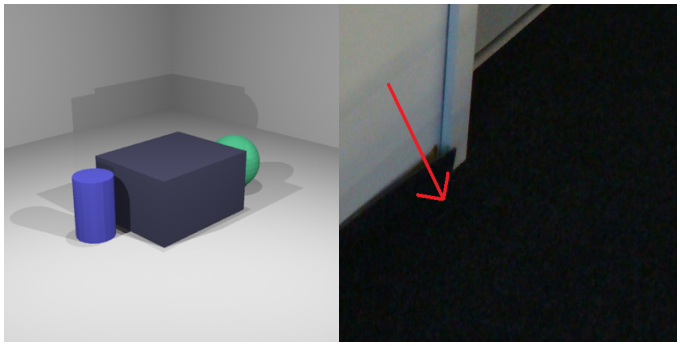

Figure 10.41: Image rendered with the material (left) and photo (right) for the material CH_gray03.

C-42 Material Sample CH_green01

Usage:

Material used for the leaves of trees and plants.

Material properties

Material Type(PBRT)	uber
Setting	Kd [0.07627 0.402 0.07627] Ks [0.03 0.03 0] Kr [0.03 0.03 0] roughness [1.0]
Diffuse component in input VRML file	[0.08627 0.702 0.08627]

The textual description in the material file

```
CH_green01 0.08627 0.702 0.08627 MAT-uber Kd [ 0.07627 0.402 0.07627 ]
                                          Ks [ 0.03 0.03 0 ]
                                          Kr [ 0.03 0.03 0 ]
                                          r [ 1.0 ]
```

Material appearance example

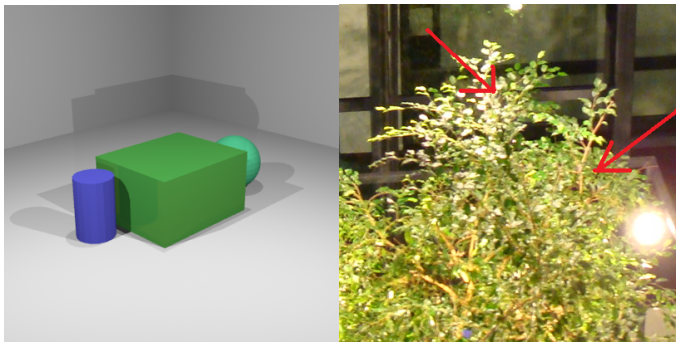

Figure 10.42: Image rendered with the material (left) and photo (right) for the material CH_green01.

C-43 Material Sample CH_metal01

Usage:

Material used for the metallic ledger-board of handrails, in particularly for the stairs and corridors.

Material properties

Material Type(PBRT)	shinymetal
Setting	roughness [1.0] Ks [0.8898 0.8898 0.8898] Kr [0.8898 0.8898 0.8898]
Diffuse component in input VRML file	[0.9298 0.9298 0.9298]

The textual description in the material file

```
CH_metal01 0.9298 0.9298 0.9298 MAT-shiny r [ 1.0 ]
                                        Ks [ 0.8898 0.8898 0.8898 ]
                                        Kr [ 0.8898 0.8898 0.8898 ]
```

Material appearance example

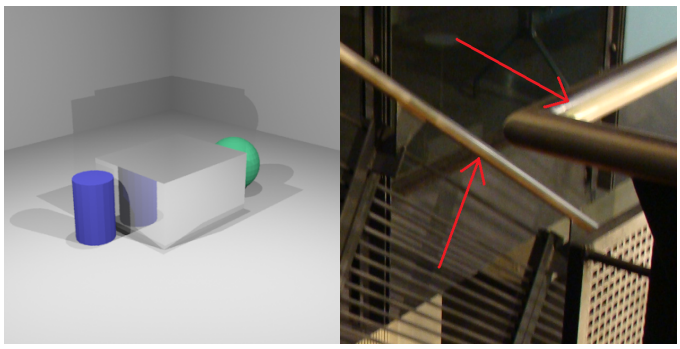

Figure 10.43: Image rendered with the material (left) and photo (right) for the material CH_metal01.

C-44 Material Sample CH_pavers01

Usage:

Material used for the tiles (flagstone) in the ground floor (perhaps granite).

Material properties

Material Type(PBRT)	uber
Setting	Kd [0.0165 0.0165 0.0475] Ks [1.0 1.0 1.0] Kr [0.0165 0.0165 0.0475]
Diffuse component in input VRML file	[0.1765 0.1765 0.2275]

The textual description in the material file

```
CH_pavers01 0.1765 0.1765 0.2275 MAT-uber Kd [ 0.0165 0.0165 0.0475 ]
                                          Ks [ 1.0 1.0 1.0 ]
                                          Kr [ 0.0165 0.0165 0.0475 ]
                                          r [ 1.0 ]
```

Material appearance example

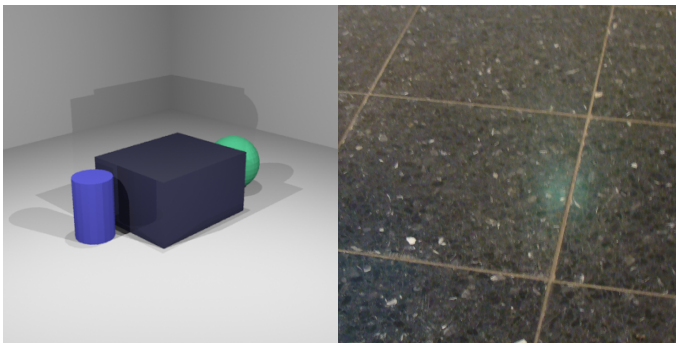

Figure 10.44: Image rendered with the material (left) and photo (right) for the material CH_pavers01.

C-45 Material Sample CH_violet01

Usage:

Material used for some walls in the ground floor.

Material properties

Material Type(PBRT)	uber
Setting	Kd [0.0547 0.01412 0.122] Ks [0.0104 0.00841 0.0112] Kr [0.0104 0.00841 0.0112] roughness [1.0]
Diffuse component in input VRML file	[0.1647 0.09412 0.3922]

The textual description in the material file

```
CH_violet01 0.1647 0.09412 0.3922 MAT-uber Kd [ 0.0547 0.01412 0.122 ]
                                           Ks [ 0.0104 0.00841 0.0112 ]
                                           Kr [ 0.0104 0.00841 0.0112 ]
                                           r [ 1.0 ]
```

Material appearance example

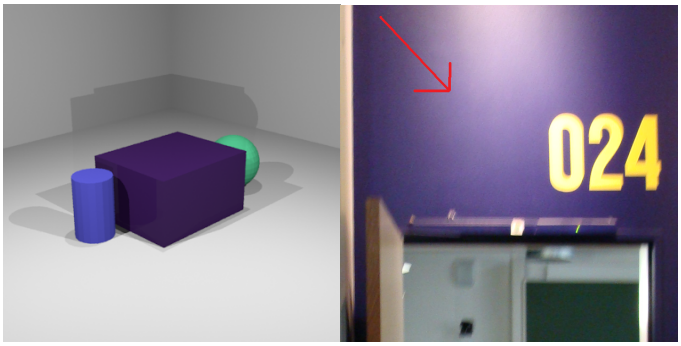

Figure 10.45: Image rendered with the material (left) and photo (right) for the material CH_violet01.

C-46 Material Sample CH_white01

Usage:

Material used for the plaster of walls in the whole building interior.

Material properties

Material Type(PBRT)	matte
Setting	sigma [31.169] Kd [0.8294 0.8294 0.8294]
Diffuse component in input VRML file	[0.7294 0.7294 0.7294]

The textual description in the material file

```
CH_white01 0.7294 0.7294 0.7294 MAT-matte s [ 31.169 ]
                                          Kd [ 0.8294 0.8294 0.8294 ]
```

Material appearance example

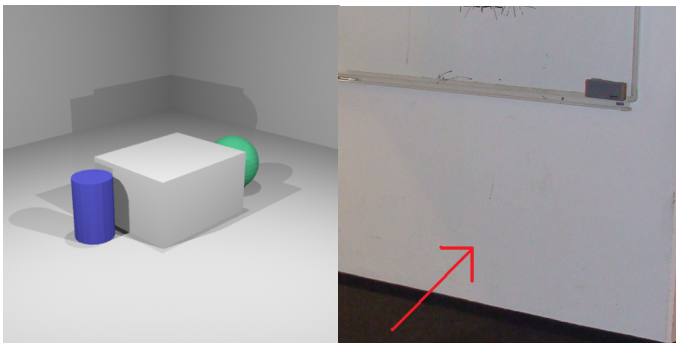

Figure 10.46: Image rendered with the material (left) and photo (right) for the material CH_white01.

C-47 Material Sample CH_white02

Usage:

Material used for the metallic frames of doors, the plastic cables isolations, the fire alarms, and some parts of fluorescent tubes.

Material properties

Material Type(PBRT)	plastic
Setting	roughness [0.9] Kd [0.9294 0.9294 0.9294] Ks [0.9294 0.9294 0.9294]
Diffuse component in input VRML file	[0.9294 0.9294 0.9294]

The textual description in the material file

```
CH_white02 0.9294 0.9294 0.9294 MAT-plastic r [ 0.9 ]
                                            Kd [ 0.9294 0.9294 0.9294 ]
                                            Ks [ 0.9294 0.9294 0.9294 ]
```

Material appearance example

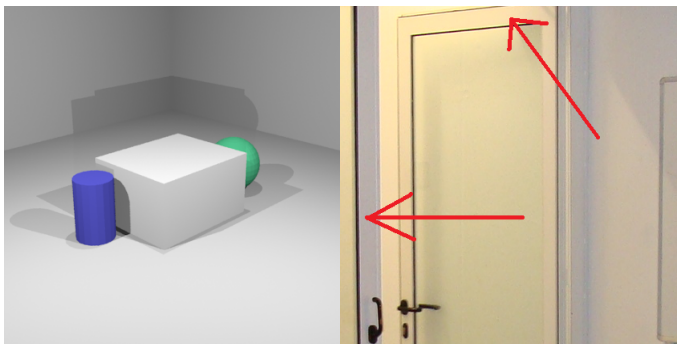

Figure 10.47: Image rendered with the material (left) and photo (right) for the material CH_white02.

C-48 Material Sample CH_white04

Usage:

Material used for the ceiling panels in the ground floor.

Material properties

Material Type(PBRT)	matte
Setting	sigma [29.2038] Kd [0.9412 0.9412 0.9412]
Diffuse component in input VRML file	[0.9412 0.9412 0.9412]

The textual description in the material file

```
CH_white04 0.9412 0.9412 0.9412 MAT-matte s [ 29.2038 ]
                                          Kd [ 0.9412 0.9412 0.9412 ]
```

Material appearance example

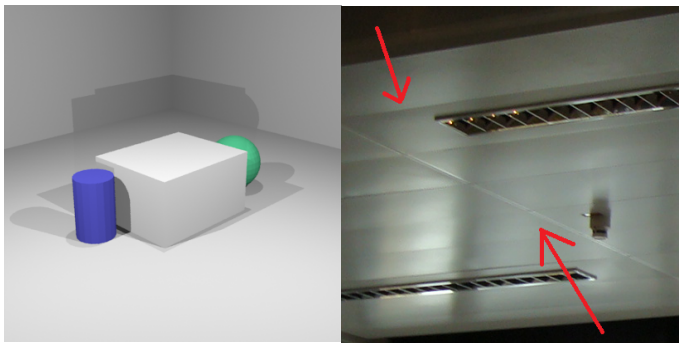

Figure 10.48: Image rendered with the material (left) and photo (right) for the material CH_white04.

C-49 Material Sample CH_white05

Usage:

Material used for the central heating bodies.

Material properties

Material Type(PBRT)	uber
Setting	roughness [1.0]
	Kd [0.9294 0.9294 0.9294] Ks [0.1 0.1 0.1] Kt [0.1 0.1 0.1]
Diffuse component in input VRML file	[0.9296 0.9296 0.9296]

The textual description in the material file

```
CH_white05 0.9296 0.9296 0.9296 MAT-uber r [ 1.0 ]
                                         Kd [ 0.9294 0.9294 0.9294 ]
                                         Ks [ 0.1 0.1 0.1 ]
                                         Kr [ 0.1 0.1 0.1 ]
```

Material appearance example

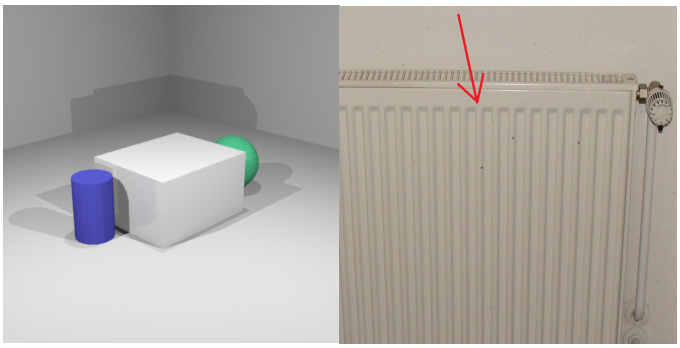

Figure 10.49: Image rendered with the material (left) and photo (right) for the material CH_white05.

C-50 Material Sample CH_yellow01

Usage:

Material used for the front revolving doors in the ground floor and for the other metallic construction outside.

Material properties

Material Type(PBRT)	matte
Setting	sigma [15.928] Kd [0.8216 0.8333 0]
Diffuse component in input VRML file	[0.9216 0.9333 0]

The textual description in the material file

```
CH\_yellow01 0.9216 0.9333 0 MAT-matte s [ 15.928 ]
                                       Kd [ 0.8216 0.8333 0 ]
```

Material appearance example

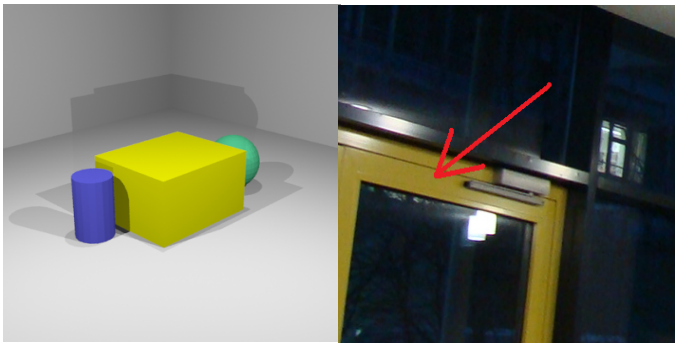

Figure 10.50: Image rendered with the material (left) and photo (right) for the material CH_yellow01.

C-51 Material Sample CH_yellow02

Usage:

Material for the wooden stair-case treads (steps) between the for the main stair-case.

Material properties

Material Type(PBRT)	matte
Setting	sigma [34.286] Kd [0.8522 0.6216 0.2353]
Diffuse component in input VRML file	[0.5922 0.5216 0.2353]

The textual description in the material file

```
CH_yellow02 0.5922 0.5216 0.2353 MAT-matte s [ 34.286 ]
                                          Kd [ 0.8522 0.6216 0.2353 ]
```

Material appearance example

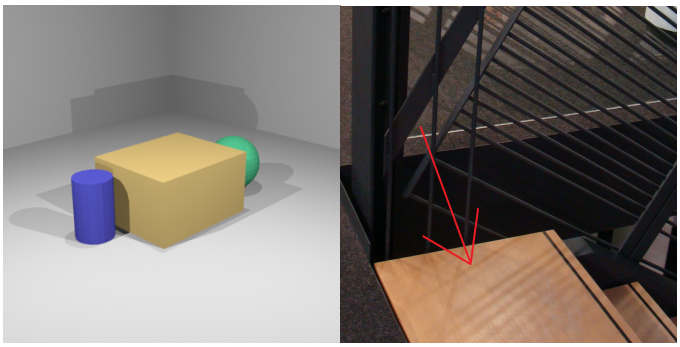

Figure 10.51: Image rendered with the material (left) and photo (right) for the material CH_yellow02.

C-52 Material Sample CH_yellow03

Usage:

Material used for the floor in the revolving doors in the ground floor.

Material properties

Material Type(PBRT)	matte
Setting	sigma [34.28] Kd [0.8078 0.651 0.2353]
Diffuse component in input VRML file	[0.8078 0.651 0.2353]

The textual description in the material file

```
CH_yellow03 0.8078 0.651 0.2353 MAT-matte s [ 34.28 ]
                                          Kd [ 0.8078 0.651 0.2353 ]
```

Material appearance example

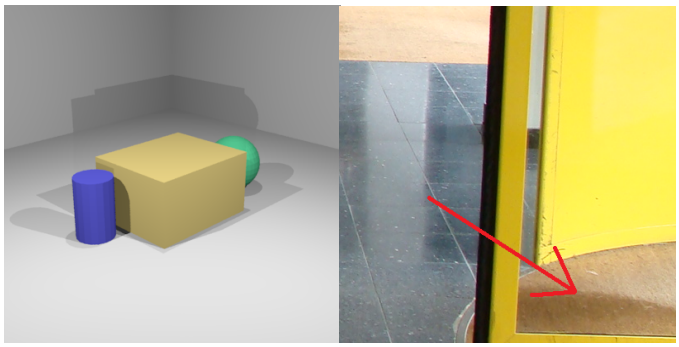

Figure 10.52: Image rendered with the material (left) and photo (right) for the material CH_yellow03.

Below you find a list of the most recent technical reports of the Max-Planck-Institut für Informatik. They are available via WWW using the URL `http://www.mpi-inf.mpg.de`. If you have any questions concerning WWW access, please contact `reports@mpi-inf.mpg.de`. Paper copies (which are not necessarily free of charge) can be ordered either by regular mail or by e-mail at the address below.

Max-Planck-Institut für Informatik
Library
attn. Anja Becker
Stuhlsatzenhausweg 85
66123 Saarbrücken
GERMANY
e-mail: `library@mpi-inf.mpg.de`

MPI-I-2009-RG1-002	P. Wischnewski, C. Weidenbach	Contextual rewriting
MPI-I-2009-5-006	S. Bedathur, K. Berberich, J. Dittrich, N. Mamoulis, G. Weikum	Scalable phrase mining for ad-hoc text analytics
MPI-I-2009-5-004	N. Preda, F.M. Suchanek, G. Kasneci, T. Neumann, G. Weikum	Coupling knowledge bases and web services for active knowledge
MPI-I-2009-5-003	T. Neumann, G. Weikum	The RDF-3X engine for scalable management of RDF data
MPI-I-2008-RG1-001	A. Fietzke, C. Weidenbach	Labelled splitting
MPI-I-2008-5-004	F. Suchanek, M. Sozio, G. Weikum	SOFI: a self-organizing framework for information extraction
MPI-I-2008-5-003	F.M. Suchanek, G. de Melo, A. Pease	Integrating Yago into the suggested upper merged ontology
MPI-I-2008-5-002	T. Neumann, G. Moerkotte	Single phase construction of optimal DAG-structured QEPs
MPI-I-2008-5-001	F. Suchanek, G. Kasneci, M. Ramanath, M. Sozio, G. Weikum	STAR: Steiner tree approximation in relationship-graphs
MPI-I-2008-4-003	T. Schultz, H. Theisel, H. Seidel	Crease surfaces: from theory to extraction and application to diffusion tensor MRI
MPI-I-2008-4-002	W. Saleem, D. Wang, A. Belyaev, H. Seidel	Estimating complexity of 3D shapes using view similarity
MPI-I-2008-1-001	D. Ajwani, I. Malinger, U. Meyer, S. Toledo	Characterizing the performance of Flash memory storage devices and its impact on algorithm design
MPI-I-2007-RG1-002	T. Hillenbrand, C. Weidenbach	Superposition for finite domains
MPI-I-2007-5-003	F.M. Suchanek, G. Kasneci, G. Weikum	Yago : a large ontology from Wikipedia and WordNet
MPI-I-2007-5-002	K. Berberich, S. Bedathur, T. Neumann, G. Weikum	A time machine for text search
MPI-I-2007-5-001	G. Kasneci, F.M. Suchanek, G. Ifrim, M. Ramanath, G. Weikum	NAGA: searching and ranking knowledge
MPI-I-2007-4-008	J. Gall, T. Brox, B. Rosenhahn, H. Seidel	Global stochastic optimization for robust and accurate human motion capture
MPI-I-2007-4-007	R. Herzog, V. Havran, K. Myszkowski, H. Seidel	Global illumination using photon ray splatting
MPI-I-2007-4-006	C. Dyken, G. Ziegler, C. Theobalt, H. Seidel	GPU marching cubes on shader model 3.0 and 4.0
MPI-I-2007-4-005	T. Schultz, J. Weickert, H. Seidel	A higher-order structure tensor
MPI-I-2007-4-004	C. Stoll, E. de Aguiar, C. Theobalt, H. Seidel	A volumetric approach to interactive shape editing
MPI-I-2007-4-003	R. Bargmann, V. Blanz, H. Seidel	A nonlinear viseme model for triphone-based speech synthesis
MPI-I-2007-4-002	T. Langer, H. Seidel	Construction of smooth maps with mean value coordinates
MPI-I-2007-4-001	J. Gall, B. Rosenhahn, H. Seidel	Clustered stochastic optimization for object recognition and pose estimation

MPI-I-2007-2-001	A. Podelski, S. Wagner	A method and a tool for automatic veriication of region stability for hybrid systems
MPI-I-2007-1-003	A. Gidenstam, M. Papatriantafilou	LFthreads: a lock-free thread library
MPI-I-2007-1-002	E. Althaus, S. Canzar	A Lagrangian relaxation approach for the multiple sequence alignment problem
MPI-I-2007-1-001	E. Berberich, L. Kettner	Linear-time reordering in a sweep-line algorithm for algebraic curves intersecting in a common point
MPI-I-2006-5-006	G. Kasnec, F.M. Suchanek, G. Weikum	Yago - a core of semantic knowledge
MPI-I-2006-5-005	R. Angelova, S. Siersdorfer	A neighborhood-based approach for clustering of linked document collections
MPI-I-2006-5-004	F. Suchanek, G. Ifrim, G. Weikum	Combining linguistic and statistical analysis to extract relations from web documents
MPI-I-2006-5-003	V. Scholz, M. Magnor	Garment texture editing in monocular video sequences based on color-coded printing patterns
MPI-I-2006-5-002	H. Bast, D. Majumdar, R. Schenkel, M. Theobald, G. Weikum	IO-Top-k: index-access optimized top-k query processing
MPI-I-2006-5-001	M. Bender, S. Michel, G. Weikum, P. Triantafilou	Overlap-aware global df estimation in distributed information retrieval systems
MPI-I-2006-4-010	A. Belyaev, T. Langer, H. Seidel	Mean value coordinates for arbitrary spherical polygons and polyhedra in $\mathbb{R}^3$
MPI-I-2006-4-009	J. Gall, J. Potthoff, B. Rosenhahn, C. Schnoerr, H. Seidel	Interacting and annealing particle filters: mathematics and a recipe for applications
MPI-I-2006-4-008	I. Albrecht, M. Kipp, M. Neff, H. Seidel	Gesture modeling and animation by imitation
MPI-I-2006-4-007	O. Schall, A. Belyaev, H. Seidel	Feature-preserving non-local denoising of static and time-varying range data
MPI-I-2006-4-006	C. Theobalt, N. Ahmed, H. Lensch, M. Magnor, H. Seidel	Enhanced dynamic reflectometry for relightable free-viewpoint video
MPI-I-2006-4-005	A. Belyaev, H. Seidel, S. Yoshizawa	Skeleton-driven laplacian mesh deformations
MPI-I-2006-4-004	V. Havran, R. Herzog, H. Seidel	On fast construction of spatial hierarchies for ray tracing
MPI-I-2006-4-003	E. de Aguiar, R. Zayer, C. Theobalt, M. Magnor, H. Seidel	A framework for natural animation of digitized models
MPI-I-2006-4-002	G. Ziegler, A. Tevs, C. Theobalt, H. Seidel	GPU point list generation through histogram pyramids
MPI-I-2006-4-001	A. Efremov, R. Mantiuk, K. Myszkowski, H. Seidel	Design and evaluation of backward compatible high dynamic range video compression
MPI-I-2006-2-001	T. Wies, V. Kuncak, K. Zee, A. Podelski, M. Rinard	On verifying complex properties using symbolic shape analysis
MPI-I-2006-1-007	H. Bast, I. Weber, C.W. Mortensen	Output-sensitive autocompletion search
MPI-I-2006-1-006	M. Kerber	Division-free computation of subresultants using bezout matrices
MPI-I-2006-1-005	A. Eigenwillig, L. Kettner, N. Wolpert	Snap rounding of Bézier curves
MPI-I-2006-1-004	S. Funke, S. Laue, R. Naujoks, L. Zvi	Power assignment problems in wireless communication
MPI-I-2005-5-002	S. Siersdorfer, G. Weikum	Automated retraining methods for document classification and their parameter tuning
MPI-I-2005-4-006	C. Fuchs, M. Goesele, T. Chen, H. Seidel	An emperical model for heterogeneous translucent objects
MPI-I-2005-4-005	G. Krawczyk, M. Goesele, H. Seidel	Photometric calibration of high dynamic range cameras
MPI-I-2005-4-004	C. Theobalt, N. Ahmed, E. De Aguiar, G. Ziegler, H. Lensch, M.A. Magnor, H. Seidel	Joint motion and reflectance capture for creating relightable 3D videos
MPI-I-2005-4-003	T. Langer, A.G. Belyaev, H. Seidel	Analysis and design of discrete normals and curvatures
MPI-I-2005-4-002	O. Schall, A. Belyaev, H. Seidel	Sparse meshing of uncertain and noisy surface scattered data